Supporting Information for

The sensitivity of ground-level ozone to precursor emissions and source contributions in Southeast Asia

Jie Hu[1,2], David C. Wong[3,4], Jiaying Li[1,2], Tingting Fang[1,5], Steve H.L. Yim[1,2,5,6*]

[1]Centre for Climate Change and Environmental Health, Nanyang Technological University, Singapore 639798, Singapore

[2]Asian School of the Environment, Nanyang Technological University, Singapore 639798, Singapore

[3]US Environmental Protection Agency, Research Triangle Park, NC, 27711, USA

[4]Department of Earth and Atmospheric Sciences, University of Houston, Houston, TX, 77204, USA

[5]Earth Observatory of Singapore, Nanyang Technological University, Singapore 639798, Singapore

[6]Lee Kong Chian School of Medicine, Nanyang Technological University, Singapore 639798, Singapore

Correspondence to: Steve H. L. Yim (yimsteve@gmail.com)

Supplementary Text S1

The WRF meteorological simulation was evaluated against the ECMWF Reanalysis v5 (ERA5) monthly mean dataset for the four monsoon seasons. The spatial patterns and quantitative comparisons of the seasonal variability of major meteorological variables are presented in Figs. S6-S9, including surface temperature, sea level pressure, and wind fields, which influenced O_3 formation and transport.

For surface temperature, the WRF simulation captured the main spatial variations across the modeling domain (Fig. S6). Statistical evaluation indicated strong agreement with ERA5, with a correlation coefficient of 0.86 and an IoA of 0.89 (Fig. S7a). The NMB between WRF and ERA5 was -4.2%, suggesting a slight regional-scale underestimation of surface temperature. For sea-level pressure, WRF showed high consistency with ERA5, yielding a correlation coefficient of 0.90 and an IoA of 0.94 (Fig. S8 and S7b), indicating that WRF reproduced sea-level pressure and associated circulation patterns over Southeast Asia. The WRF-simulated wind fields were also generally consistent with ERA5 in terms of both prevailing flow direction and wind speed (Fig. S9). Quantitatively, the wind evaluation showed a reasonably strong spatial correlation of 0.81 and an IoA of 0.88 (Fig. S7c and S7d), demonstrating that WRF captured the spatial variability of near-surface wind patterns. Overall, the meteorological evaluations showed good consistency between WRF and ERA5 across all monsoon seasons, indicating that WRF results reasonably represented the dominant monsoon-related characteristics over Southeast Asia and supported subsequent air quality modeling.

Supplementary Figures

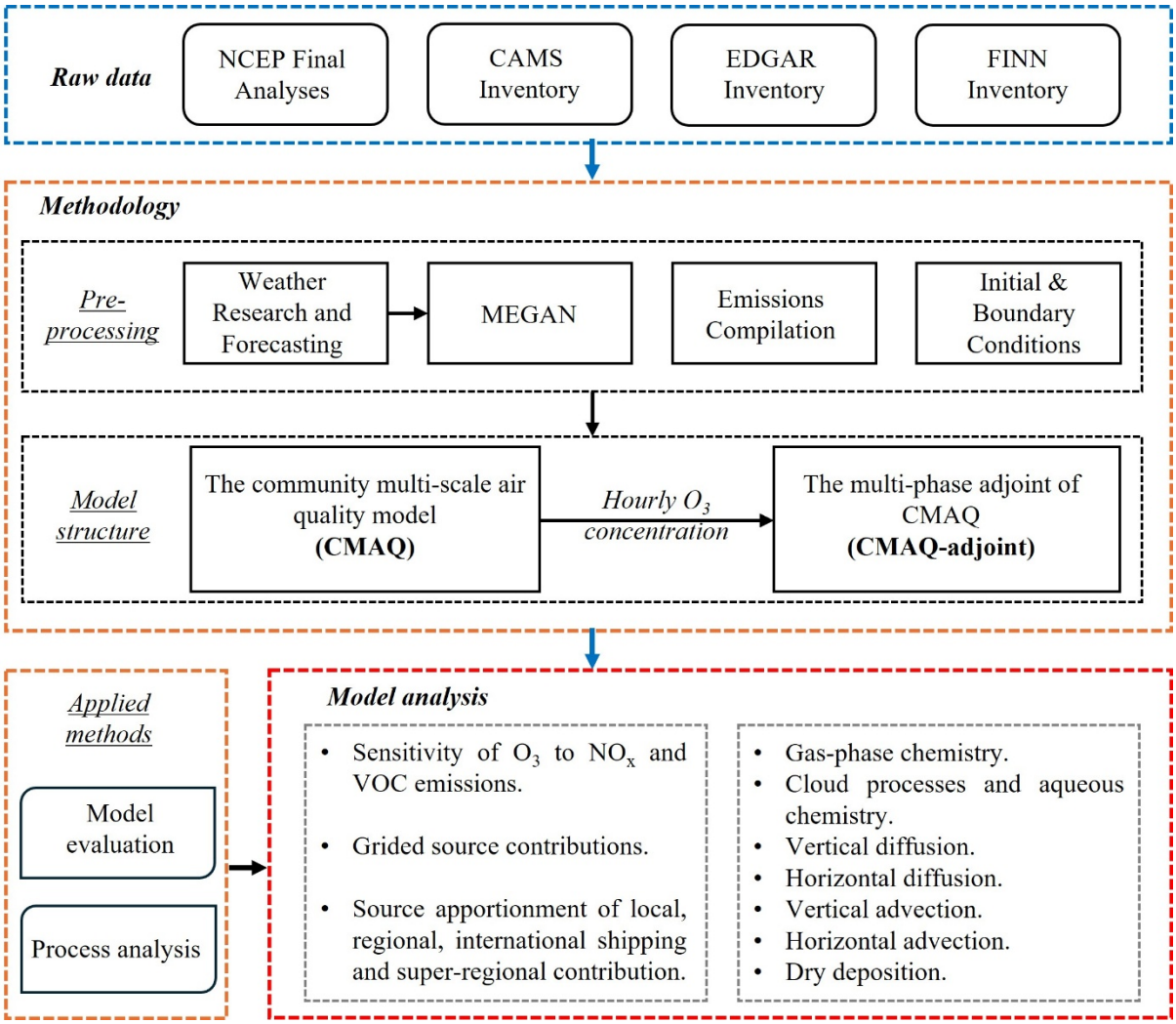

Fig. S1. The schematic flowchart of the study.

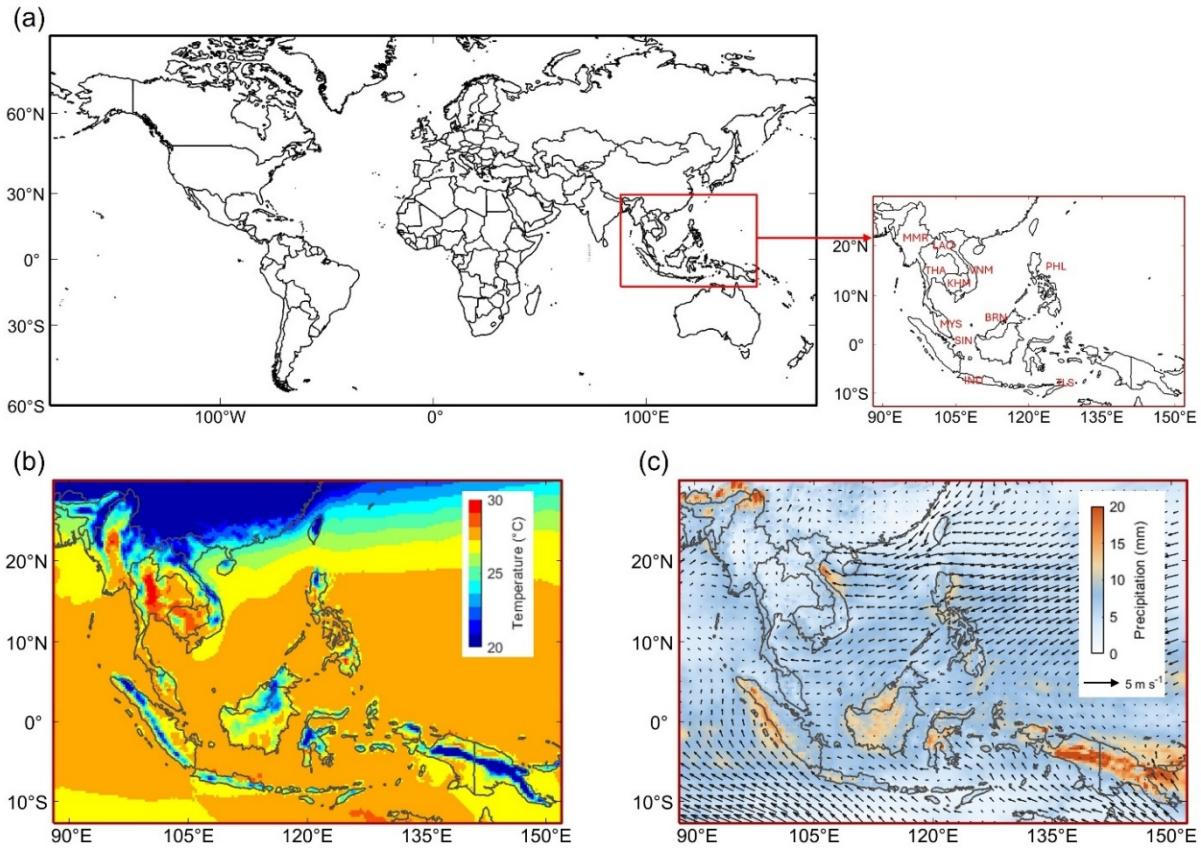

Fig. S2. Study domain and climatological characteristics of Southeast Asia. (a) The geographic location of the Southeast Asia study domain is highlighted on the global map, with country boundaries indicated. (b) Annual mean near-surface air temperature (°C) over Southeast Asia. (c) Annual accumulated precipitation (mm) and mean near-surface wind fields (m s^{-1}) over Southeast Asia. SIN: Singapore, MYS: Malaysia, IDN: Indonesia, BRN: Brunei, PHL: Philippines, VNM: Vietnam, KHM: Cambodia, THA: Thailand, LAO: Laos, MMR: Myanmar, TLS: East Timor.

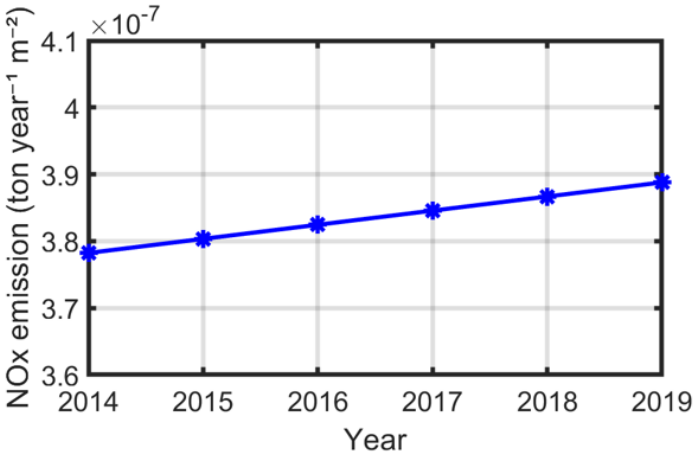

Fig. S3. The regional-mean NO_x emissions in Southeast Asia during 2014-2023. The 2019 emissions exhibited only small interannual variability (within approximately 0.5% per year) during 2014-2019.

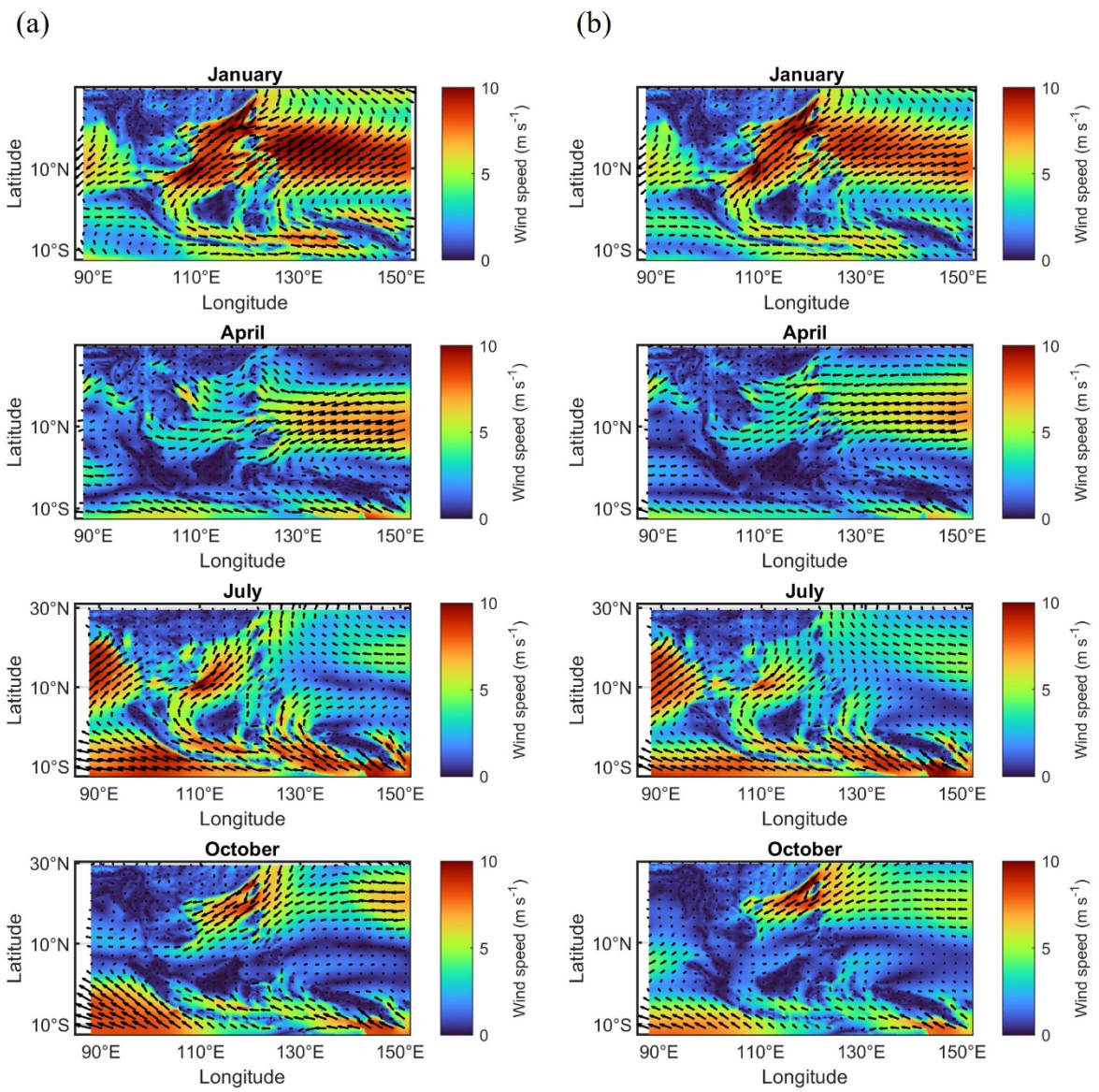

Fig. S4. The wind field in the four monsoon seasons in (a) 2019 and (b) 2014-2023 in Southeast Asia.

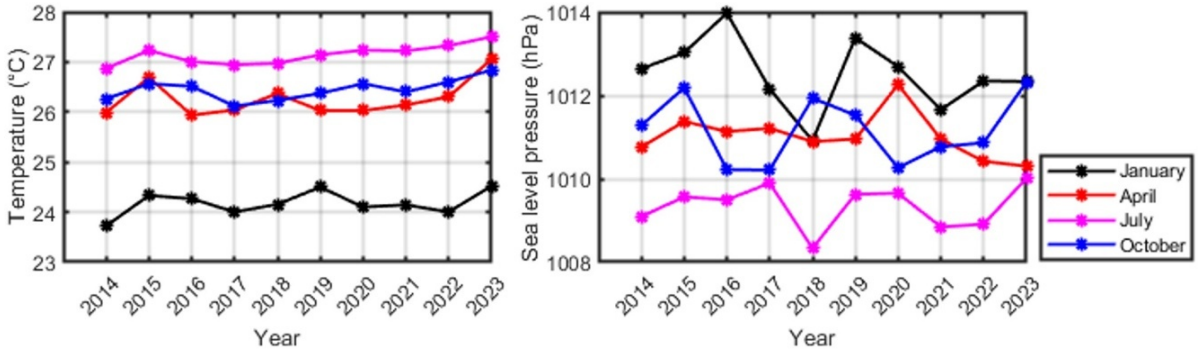

Fig. S5. The regional-mean surface temperature and sea level pressure in Southeast Asia during 2014-2023.

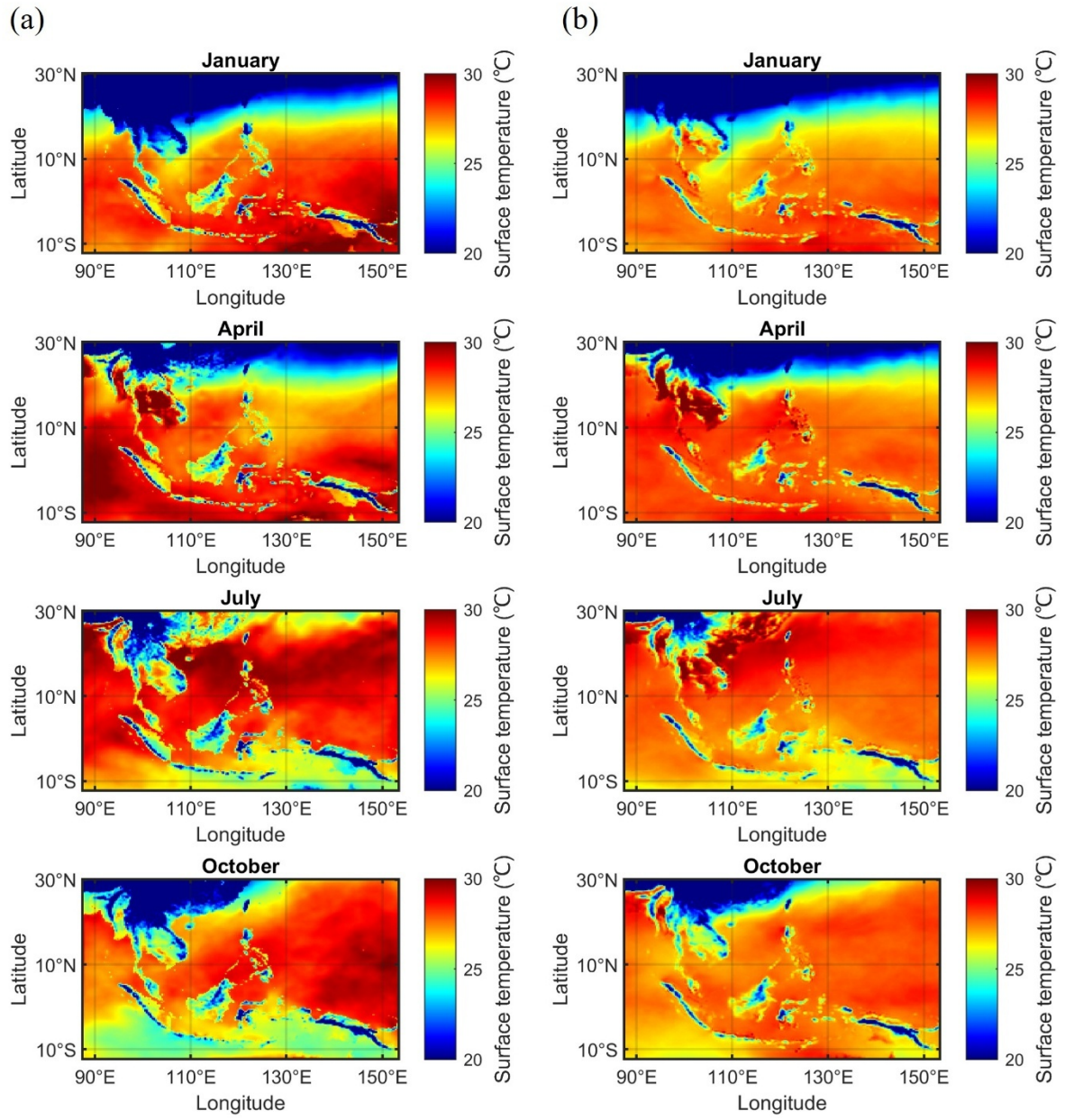

Fig. S6. Spatial comparison between the (a) simulated surface temperature and (b) the ERA5 reanalysis data in the four monsoon seasons in Southeast Asia.

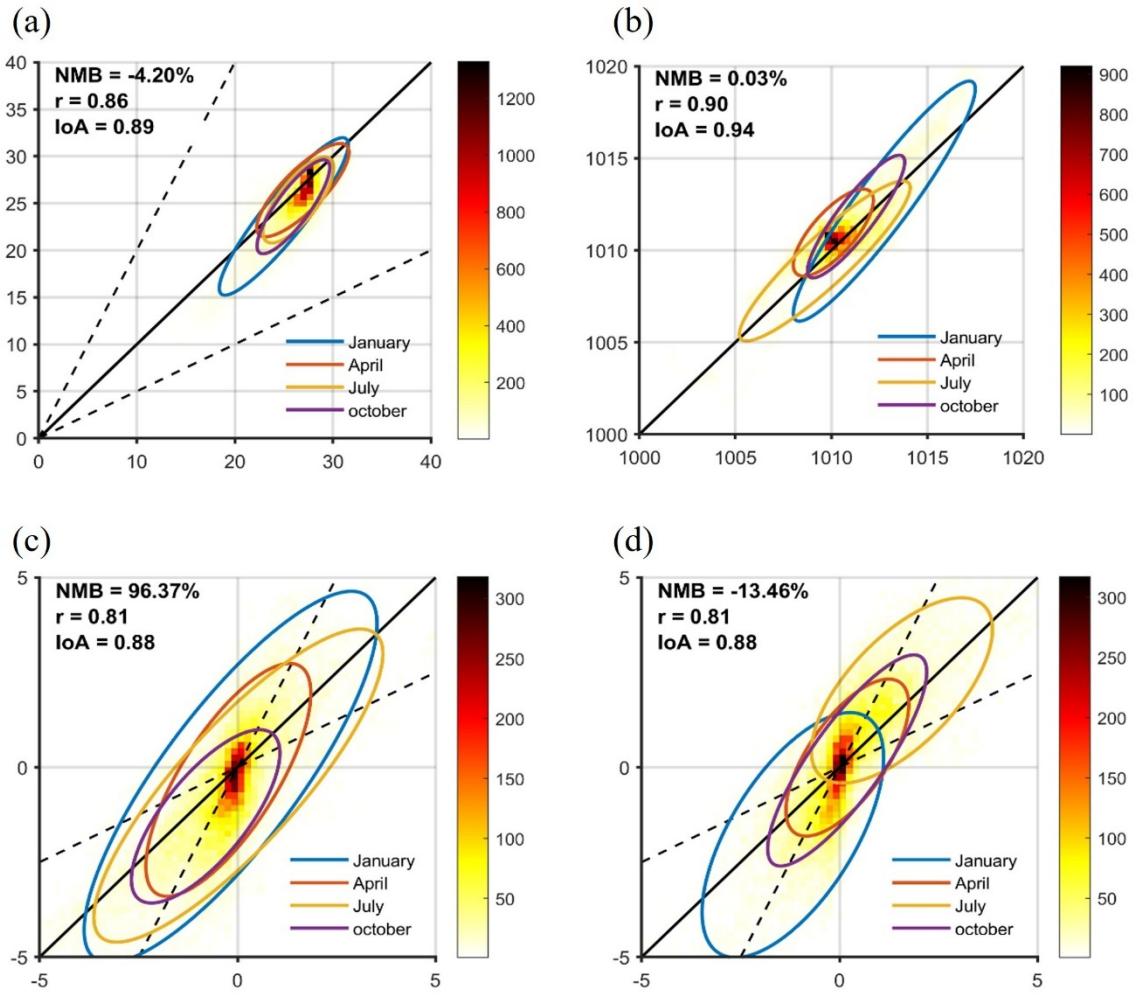

Fig. S7. Comparison between WRF simulation and the ERA5 reanalysis data for (a) surface temperature, (b) sea level pressure, (c) wind field horizontal direction, and (d) wind field vertical direction.

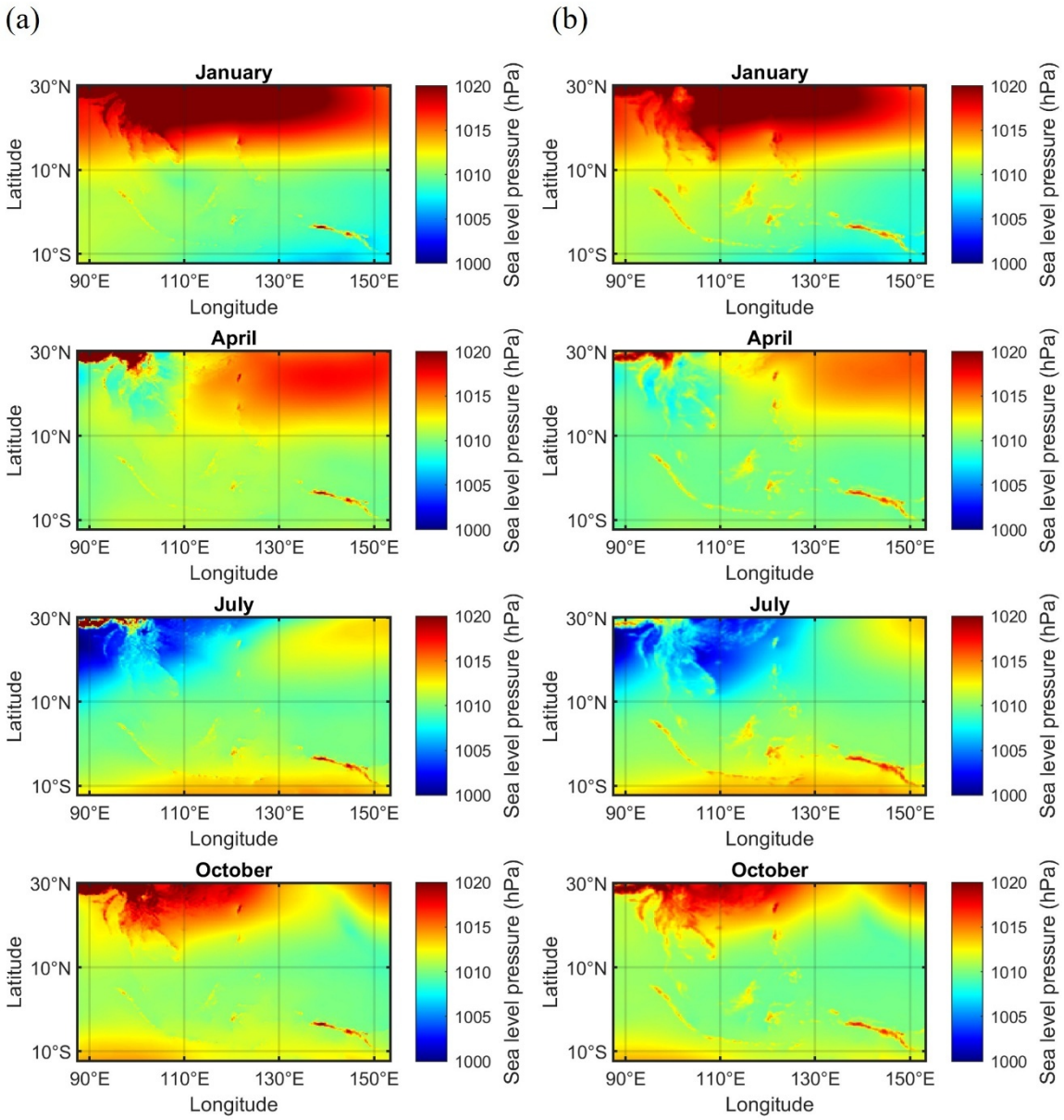

Fig. S8. Spatial comparison between the (a) simulated sea level pressure and the (b) ERA5 reanalysis data in the four monsoon seasons in Southeast Asia.

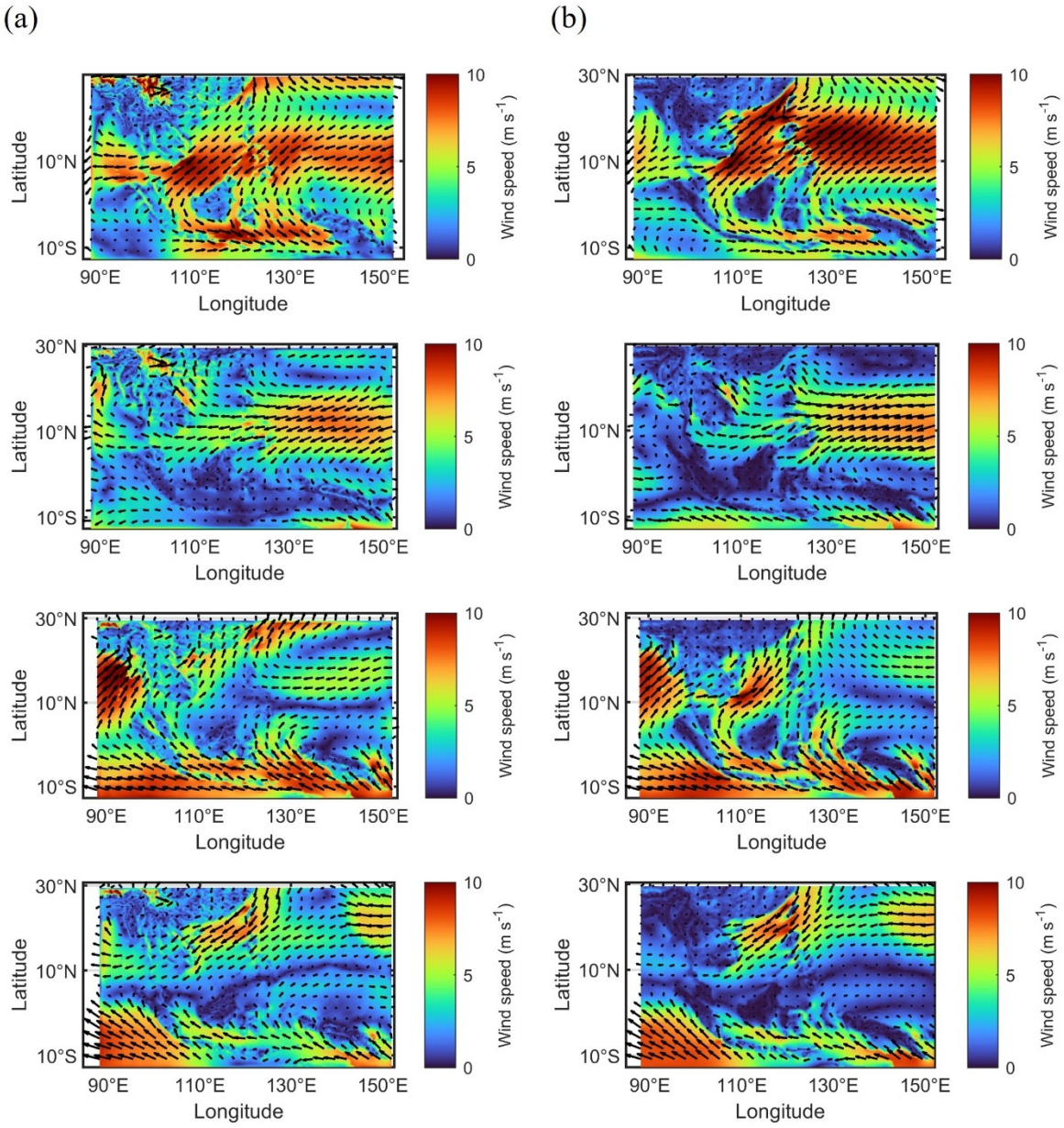

Fig. S9. Spatial comparison between the (a) simulated wind field and the (b) ERA5 reanalysis data in the four monsoon seasons in Southeast Asia.

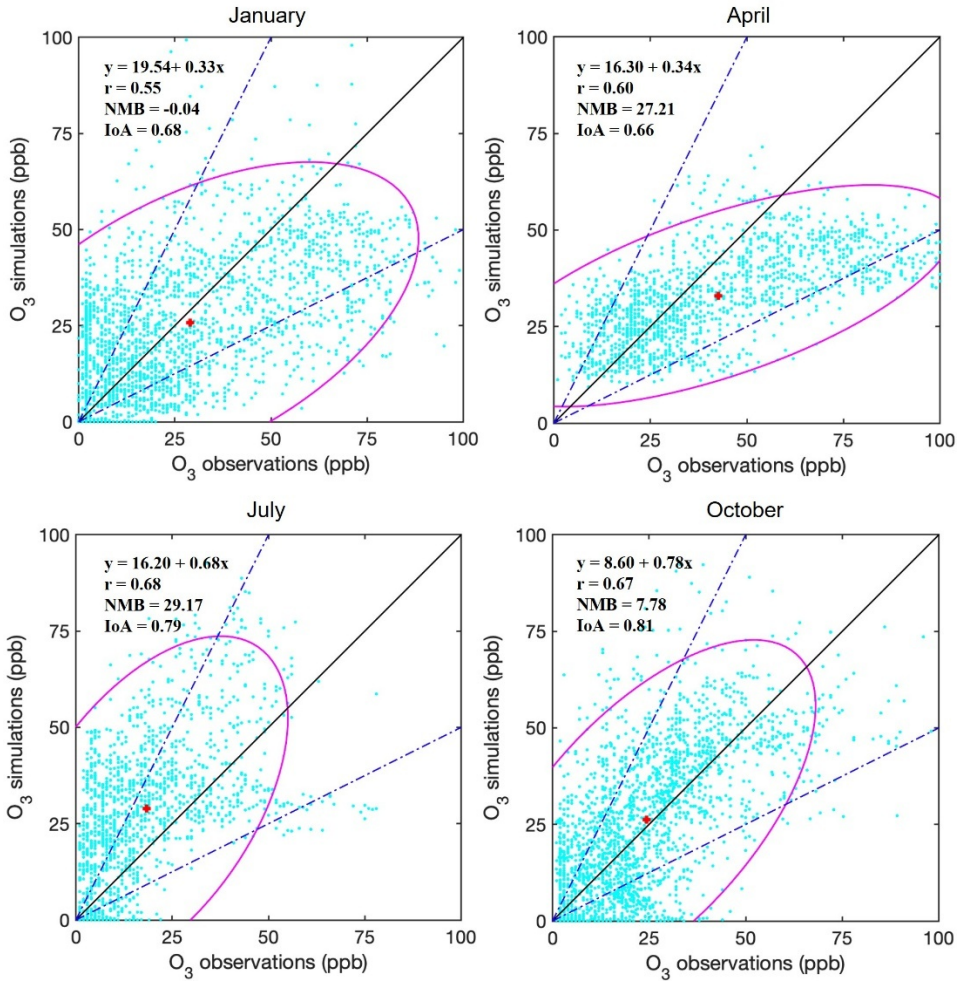

Fig. S10. CMAQ model evaluation by comparing the O_3 simulation with the observation data from monitoring stations. The ellipses represent the 95% confidence interval of the scatter points, and the centroid crosses show the median value. The statistical indicators (r, NMB (%), and IoA) were calculated using all the comparison data from available stations. The 1:1 line denotes the perfect predictions, and the 2:1 and 0.5:1 lines represent the ±50% simulations, respectively.

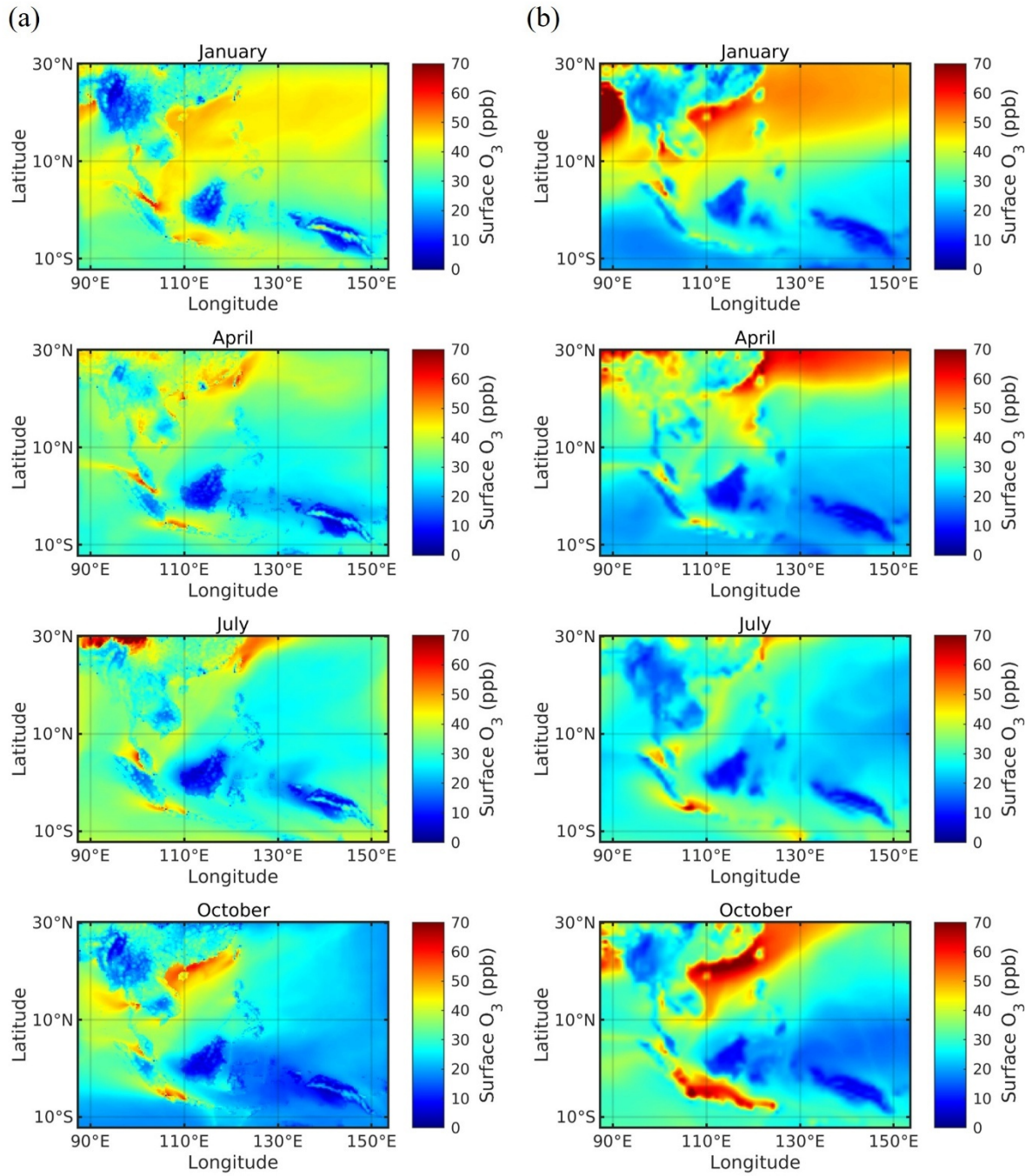

Fig. S11. Spatial comparison between CMAQ simulation and the CAMS EAC4 reanalysis data in the four monsoon seasons.

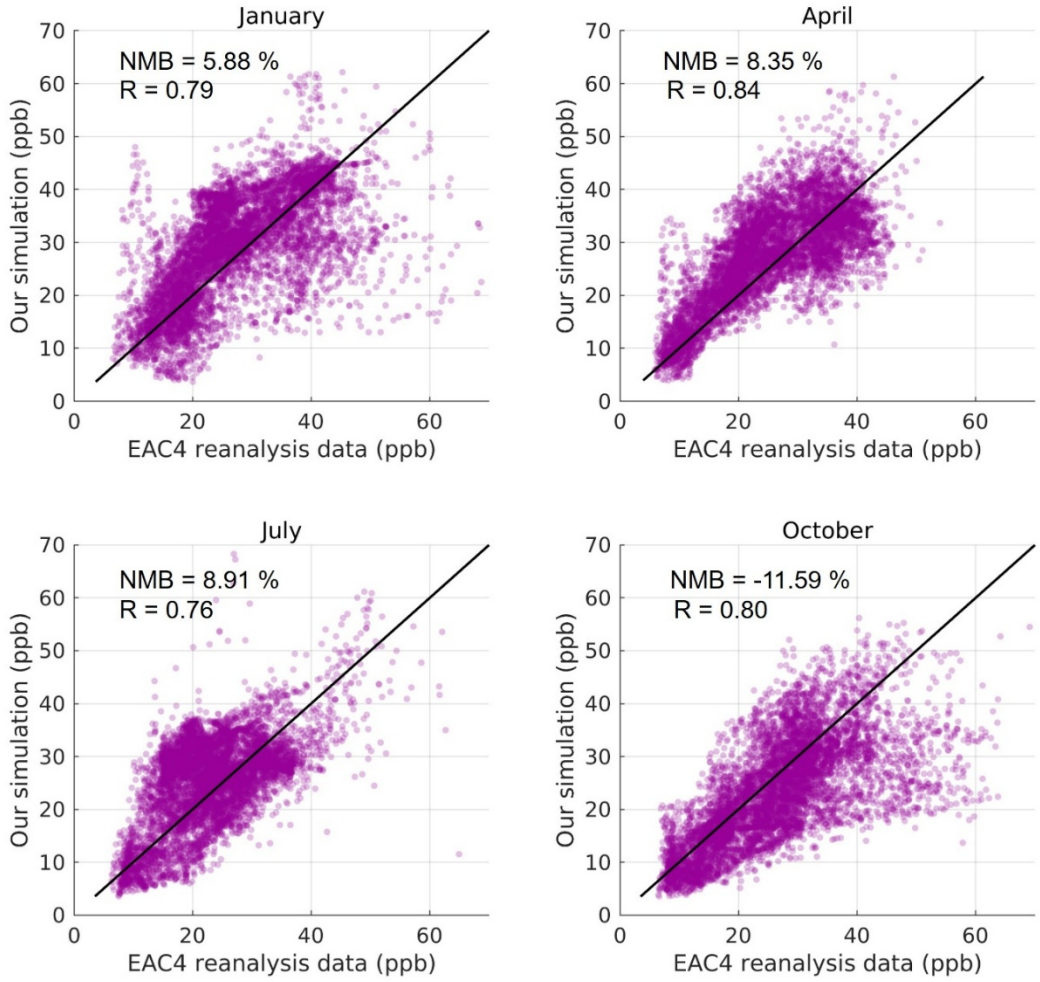

Fig. S12. Evaluation between the CMAQ simulation and the CAMS EAC4 reanalysis data in the four monsoon seasons.

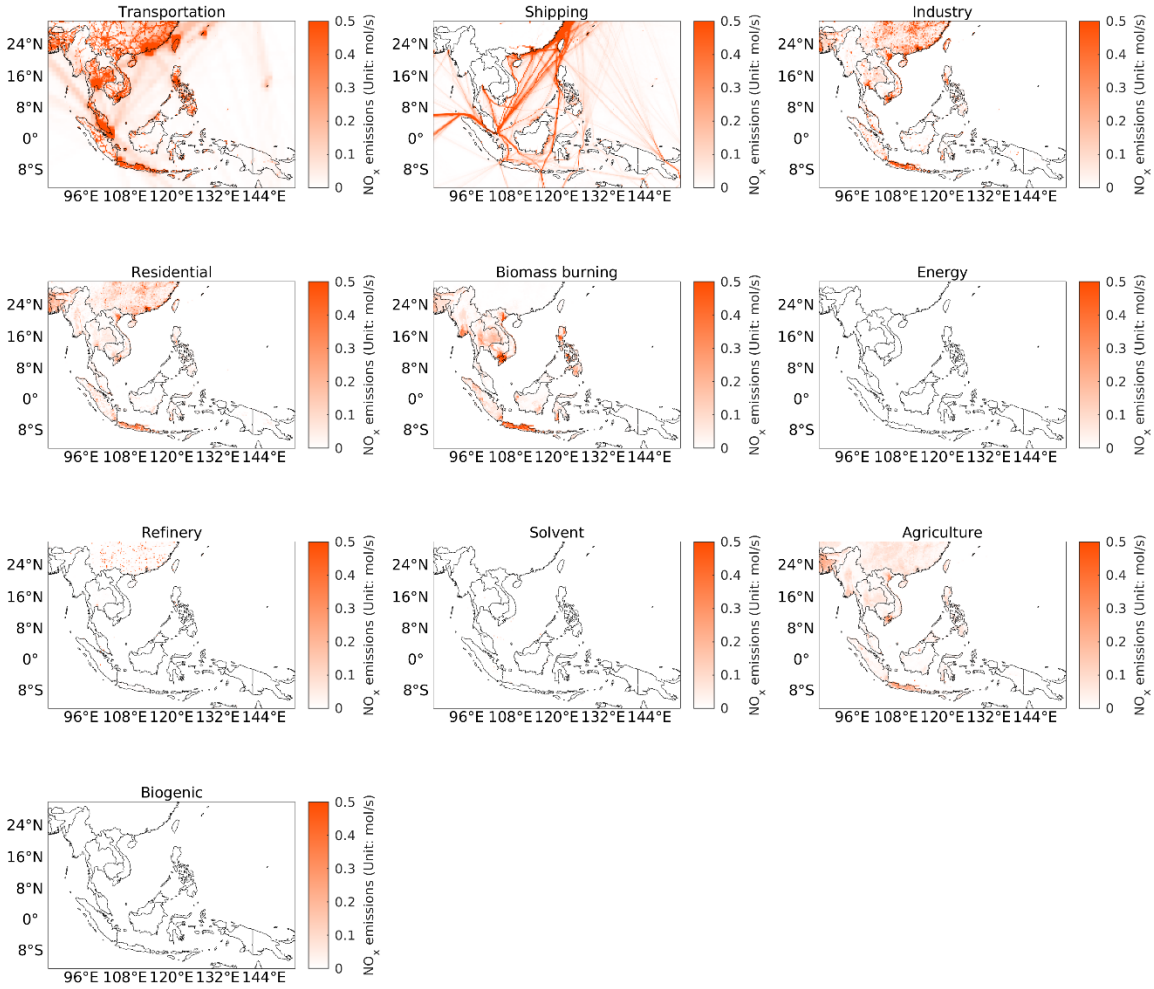

Fig. S13. Spatial distribution of NO_x emissions from different sectors in Southeast Asia.

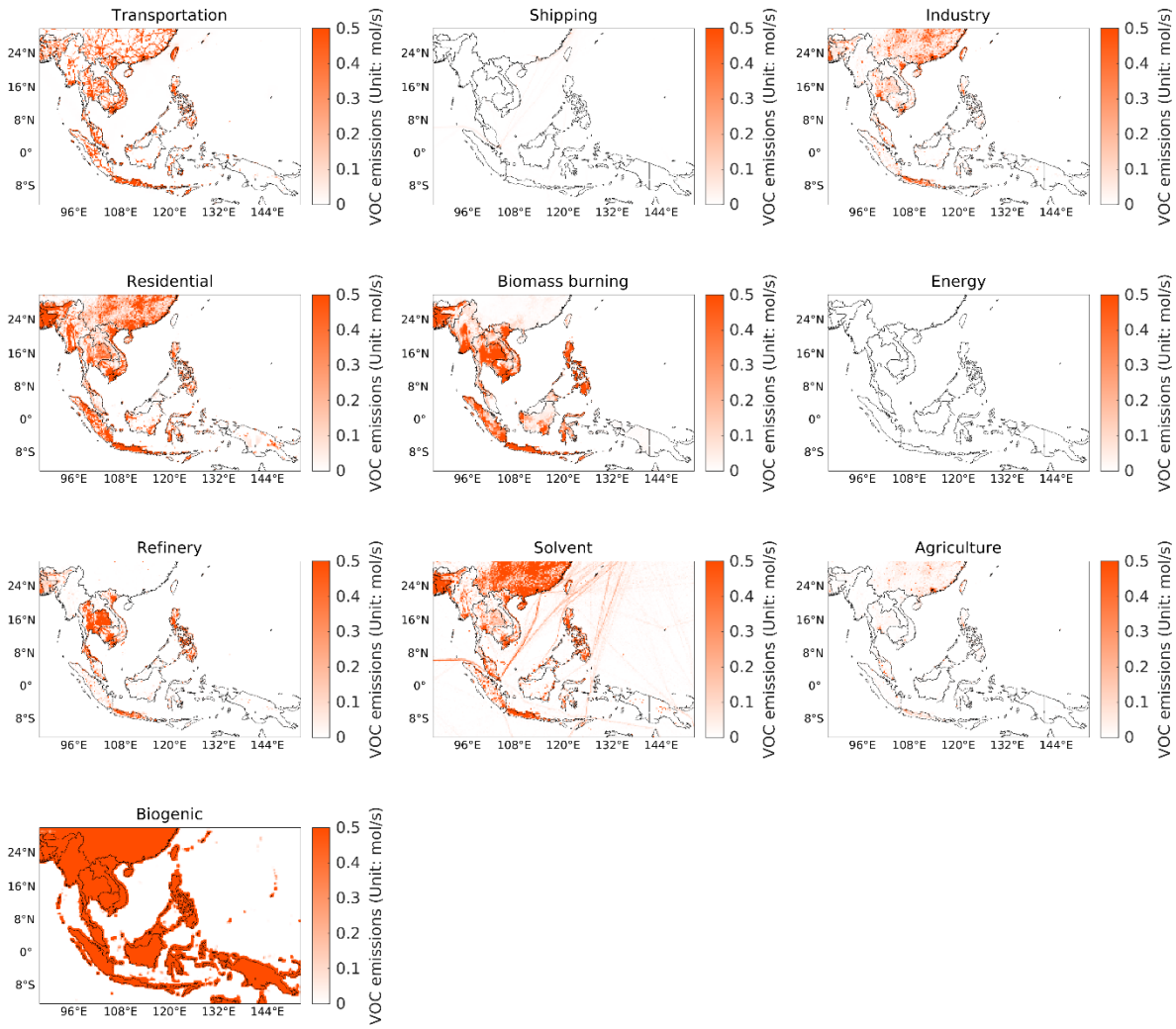

Fig. S14. Spatial distribution of VOC emissions from different sectors in Southeast Asia.

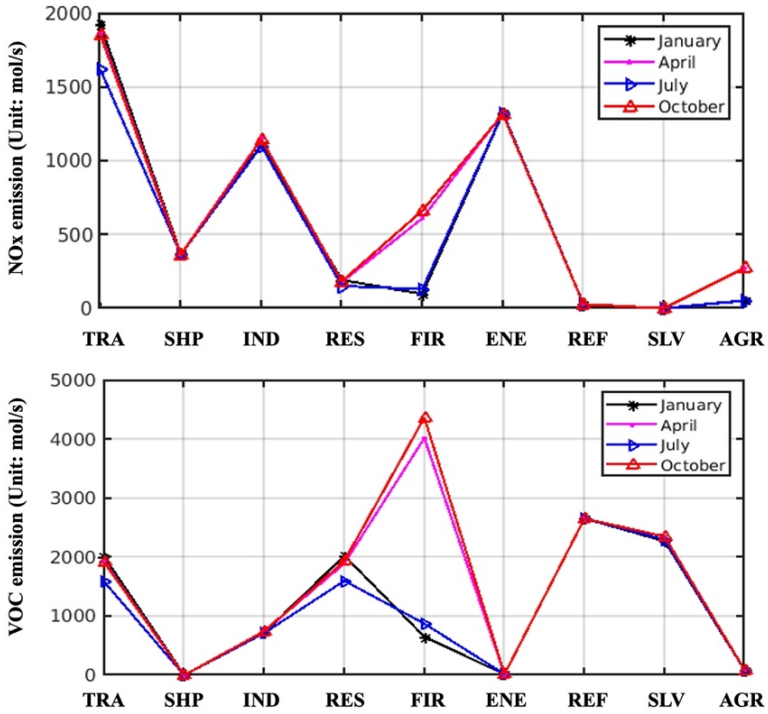

Figure S15. NO_x and VOC emissions for Southeast Asia from nine different anthropogenic sectors during four monsoon seasons. TRA: transportation, SHP: shipping, IND: industrial processes, RES: residential, FIR: biomass burning (fire), ENE: power generation, REF: refineries, SLV: solvent and fugitives, AGR: agricultural sources.

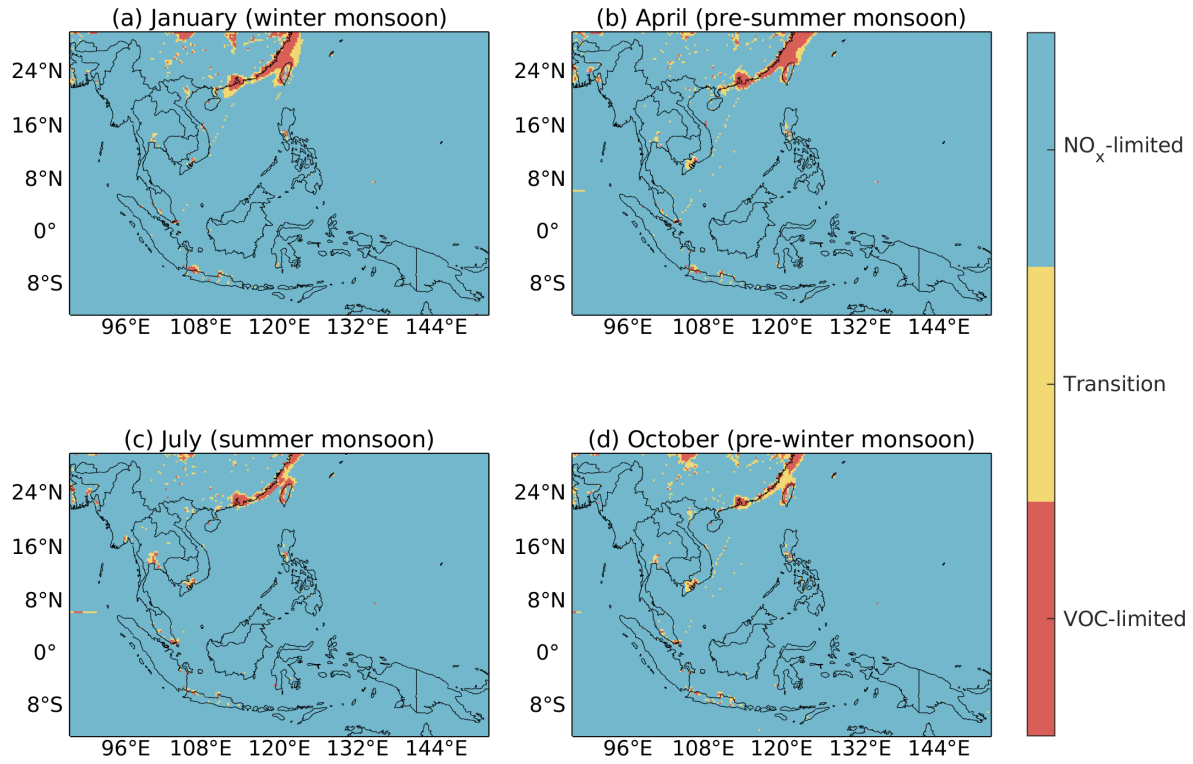

Fig. S16. Spatial distribution of the O_3 formation regimes over Southeast Asia during winter, pre-summer, summer, and pre-winter monsoon by the simulated ground-level CH_2O/NO_2. The VOC-limited regime (<0.4), the transition regime (0.4-0.7), and the NO_x-limited regime (>0.7) are defined, according to (Jin et al., 2017).

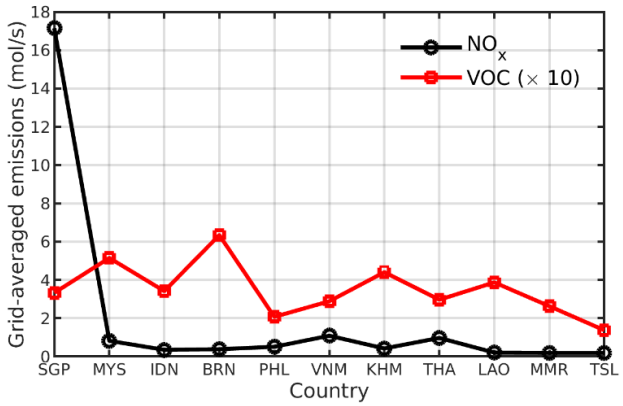

Fig. S17. Grid-averaged NO_x and VOC emissions in the countries in Southeast Asia.

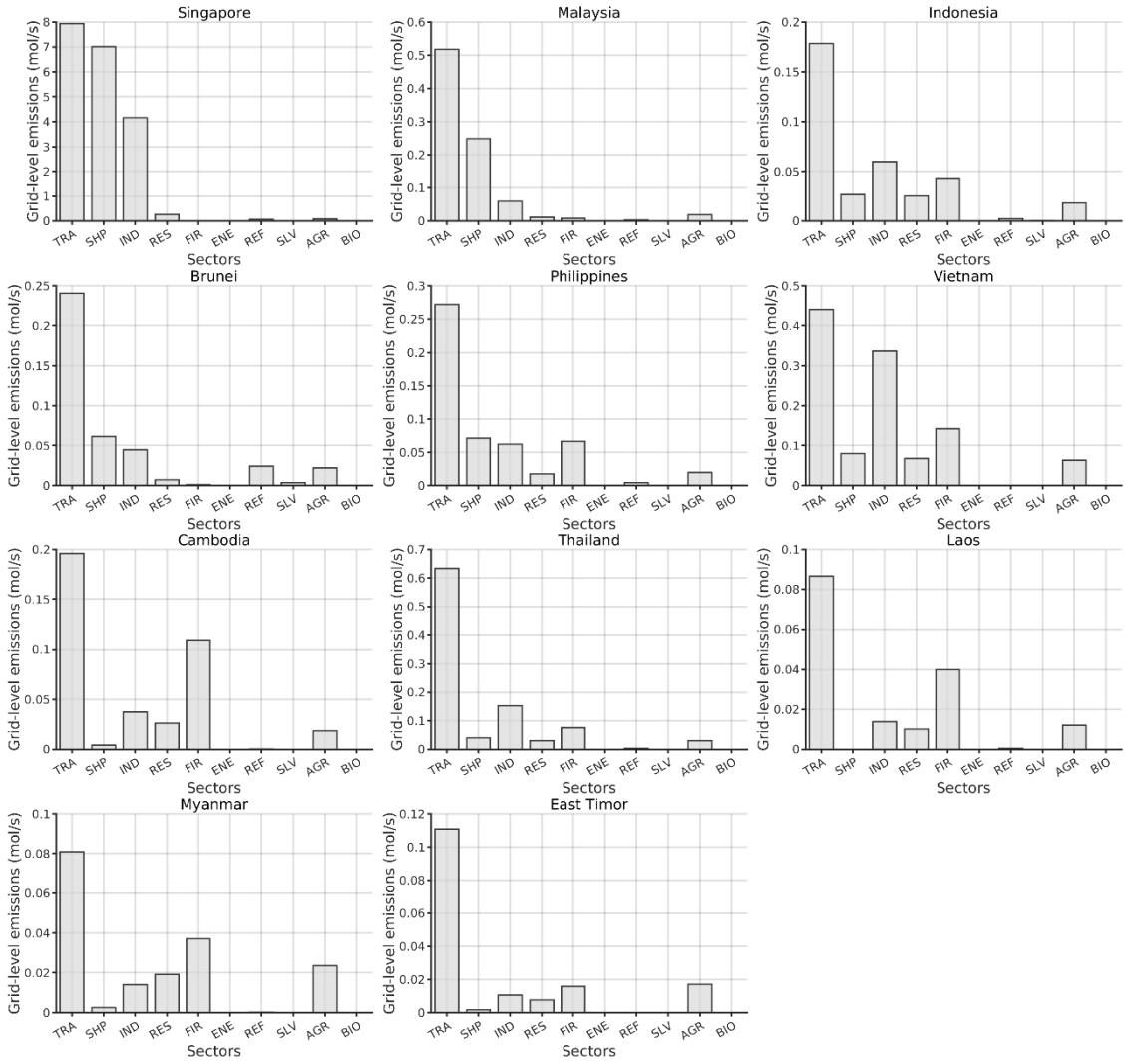

Fig. S18. Statistics of grid-level NO_x emissions from different sectors in Southeast Asia. TRA: transportation, SHP: shipping, IND: industry, RES: residential, FIR: fire, ENE: energy, REF: refinery, SLV: solvent, AGR: agriculture, BIO: biogenic emissions.

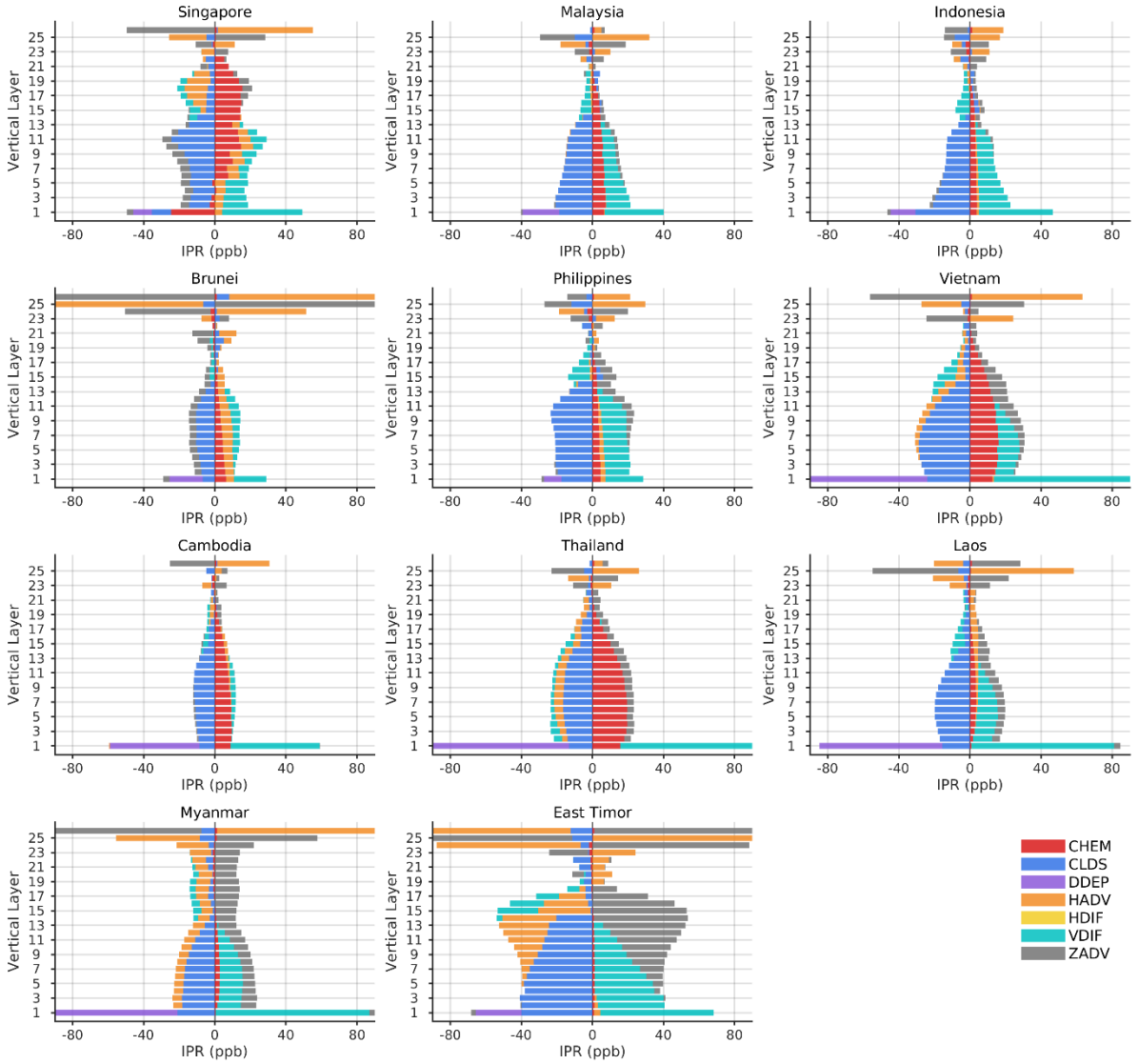

Fig. S19. The hourly averaged vertical distribution of the 26 layers from IPR analysis during the four monsoon seasons.

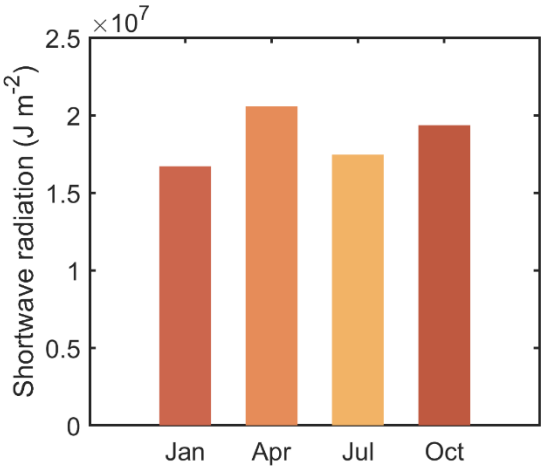

Fig. S20. Averaged short-wave radiation during the four monsoon seasons in 2019 in Southeast Asia.

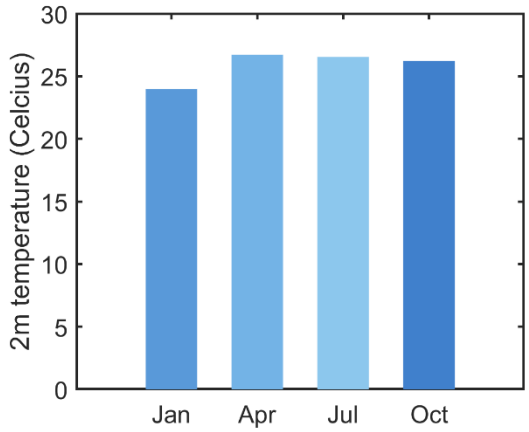

Fig. S21. Averaged 2m-temperature during the four monsoon seasons in 2019 in Southeast Asia.

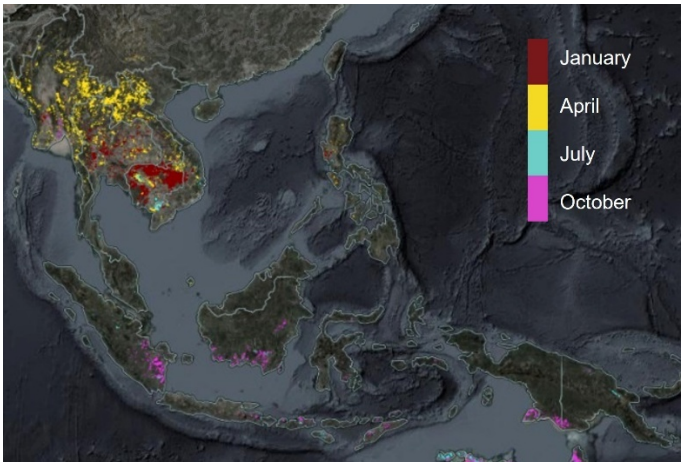

Fig. S22. MODIS burned areas in the four monsoon seasons in Southeast Asia in 2019. Downloaded from: https://firms.modaps.eosdis.nasa.gov/

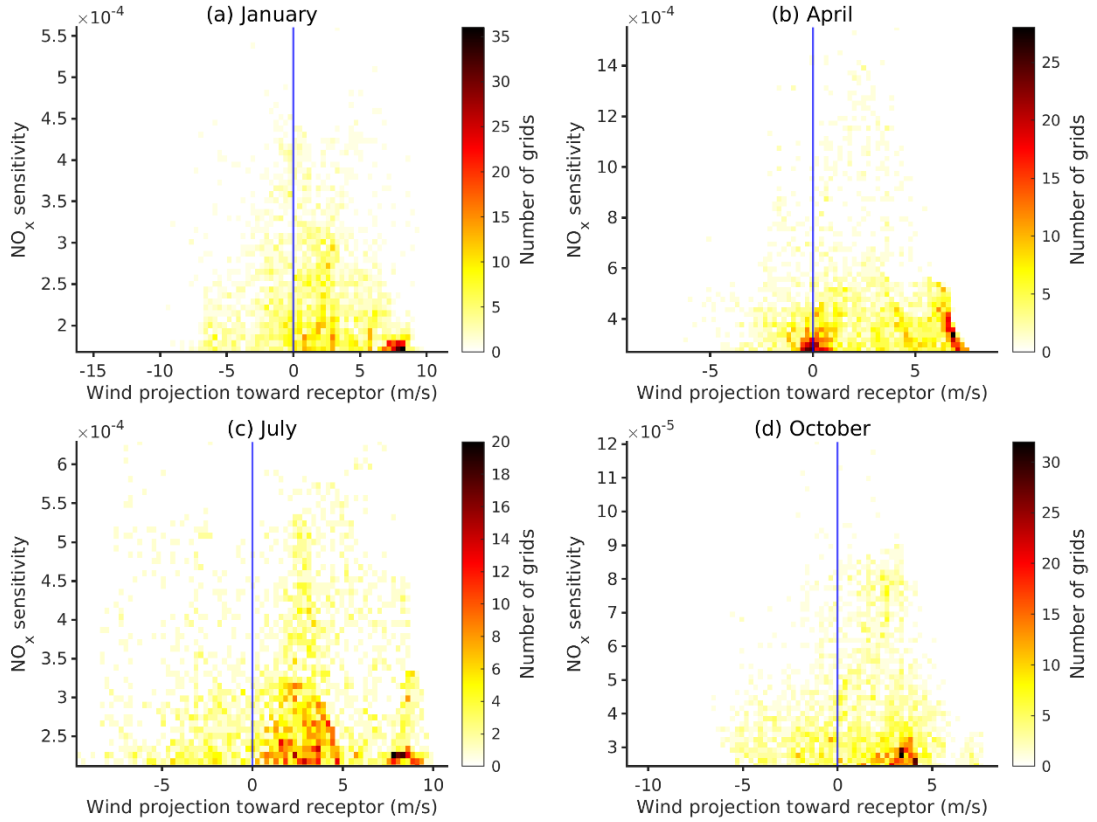

Fig. S23. Statistics of NO_x sensitivity signals in the upwind and downwind areas toward Southeast Asia.

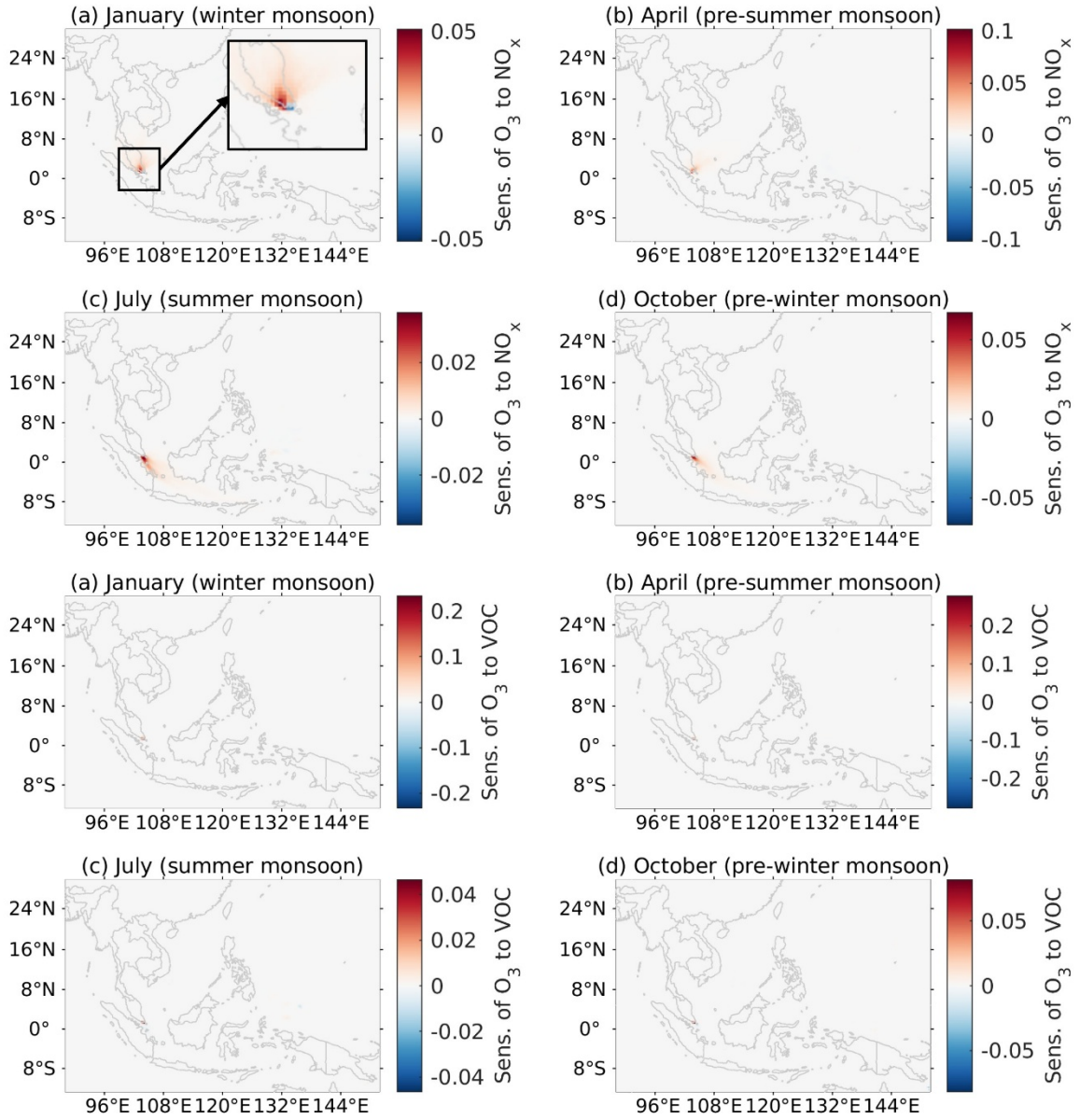

Fig. S24. Spatial distribution of the monthly mean sensitivity of O_3 in Singapore to NO_x and VOC emissions during the four monsoon seasons.

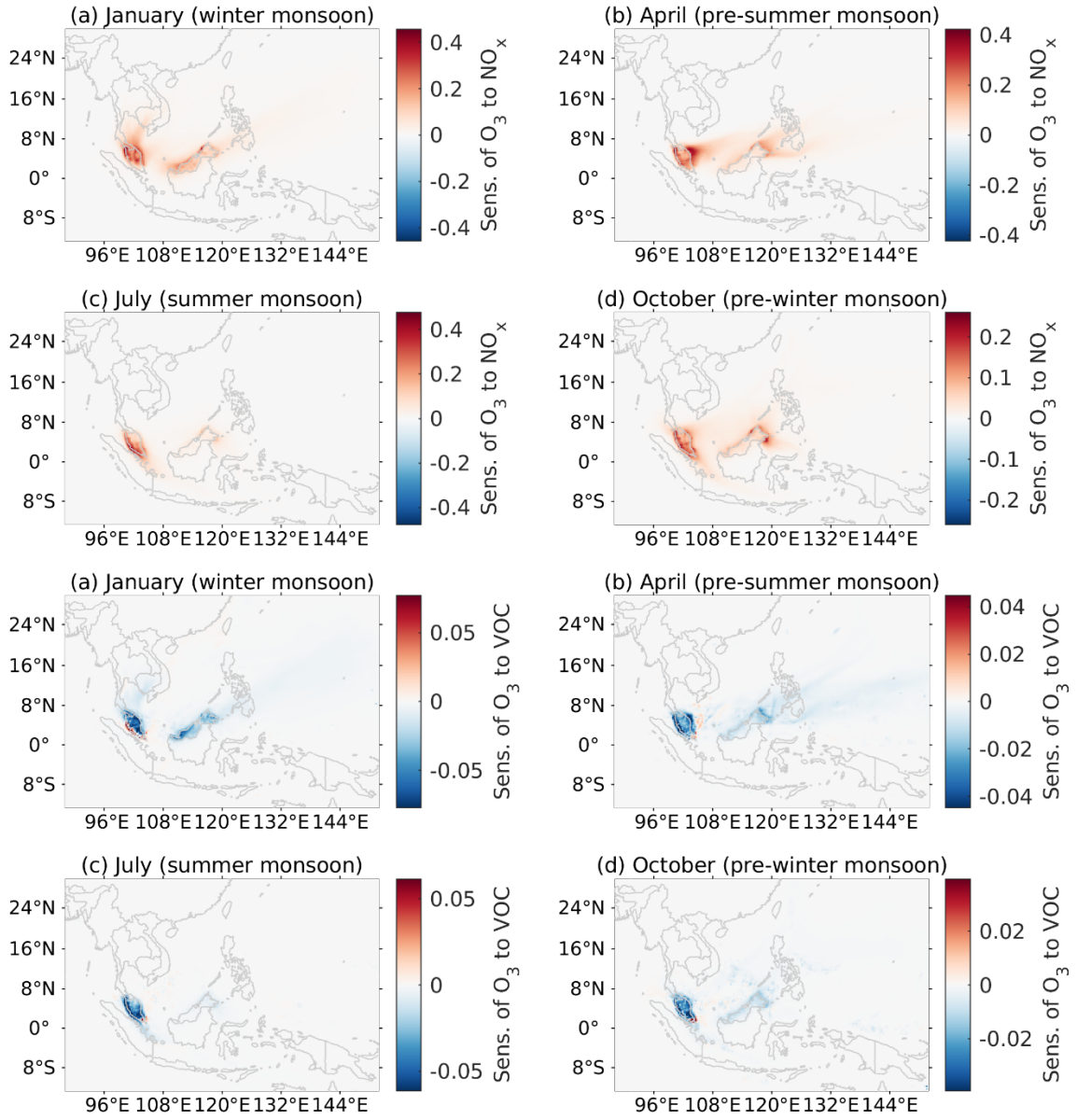

Fig. S25. Spatial distribution of the monthly mean sensitivity of O_3 in Malaysia to NO_x and VOC emissions during the four monsoon seasons.

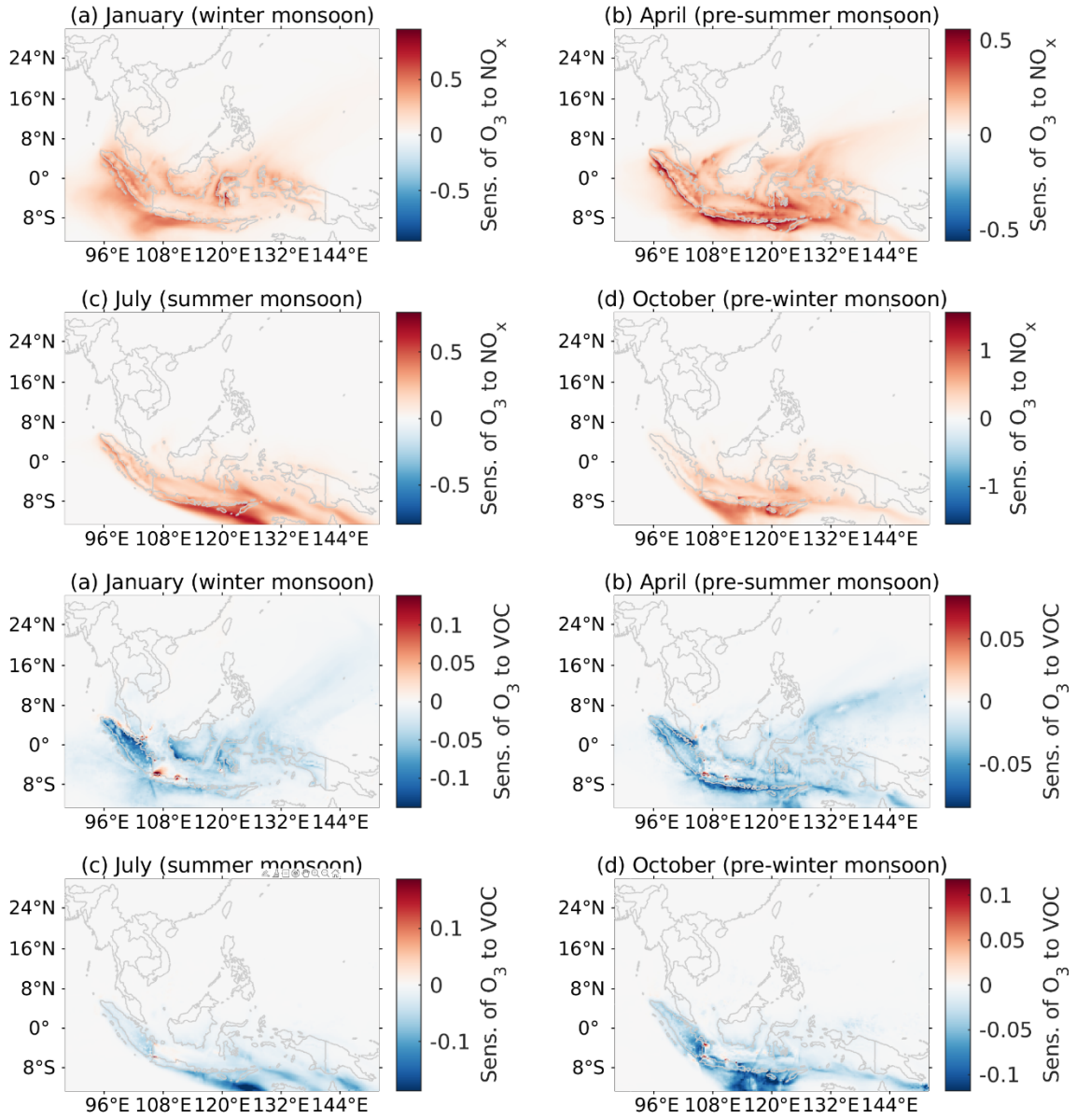

Fig. S26. Spatial distribution of the monthly mean sensitivity of O_3 in Indonesia to NO_x and VOC emissions during the four monsoon seasons.

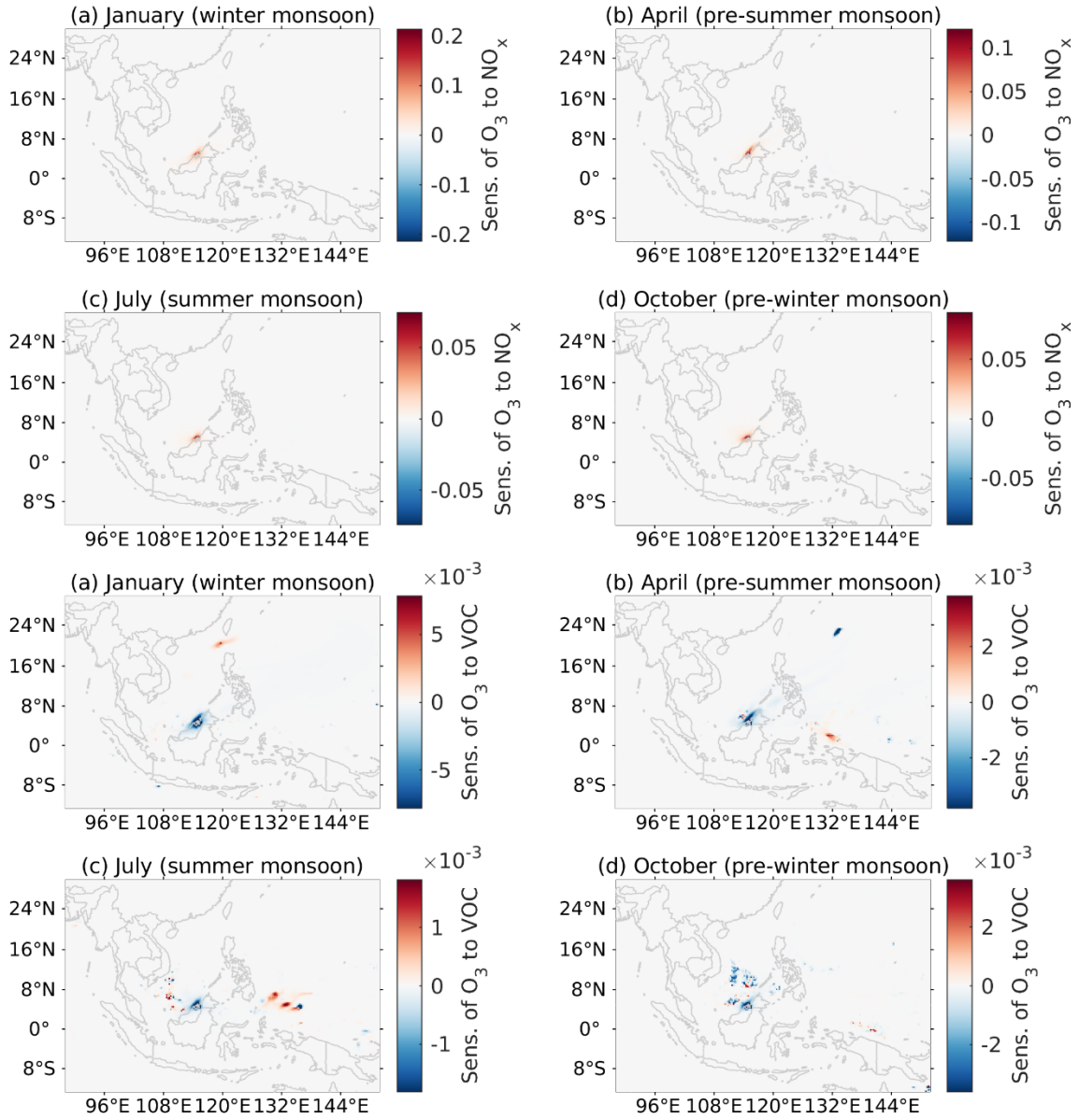

Fig. S27. Spatial distribution of the monthly mean sensitivity of O_3 in Brunei to NO_x and VOC emissions during the four monsoon seasons.

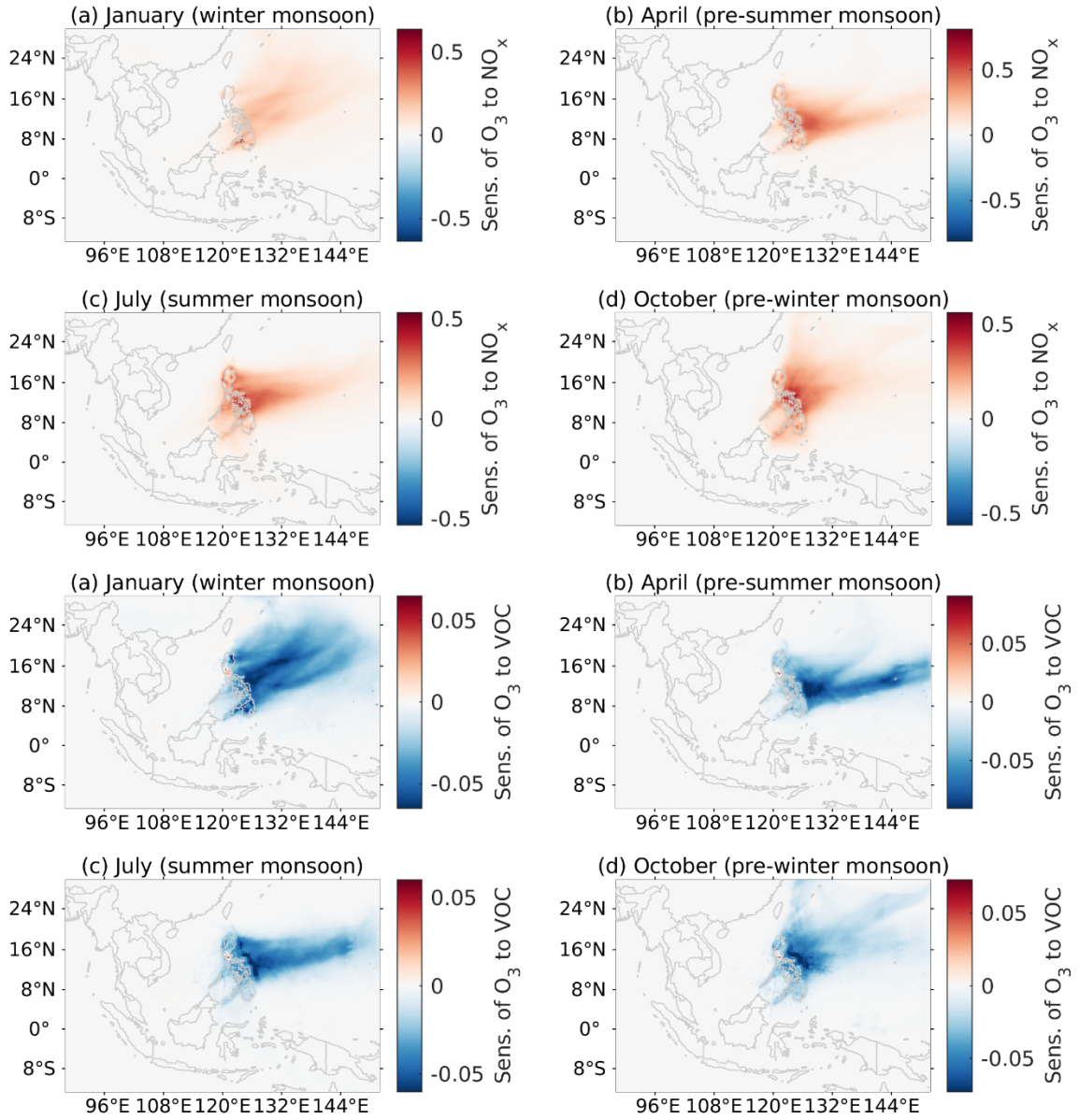

Fig. S28. Spatial distribution of the monthly mean sensitivity of O_3 in the Philippines to NO_x and VOC emissions during the four monsoon seasons.

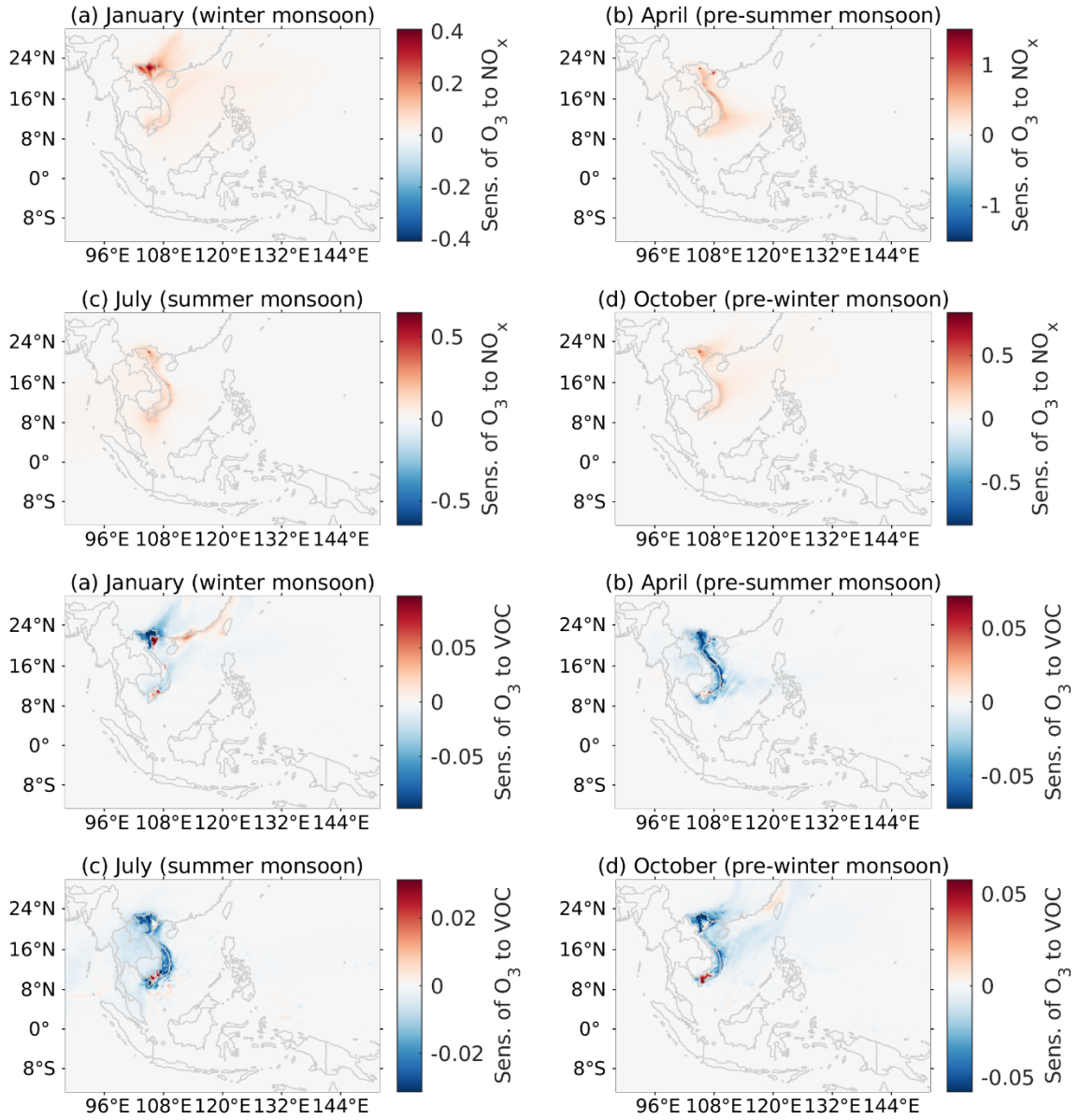

Fig. S29. Spatial distribution of the monthly mean sensitivity of O_3 in Vietnam to NO_x and VOC emissions during the four monsoon seasons.

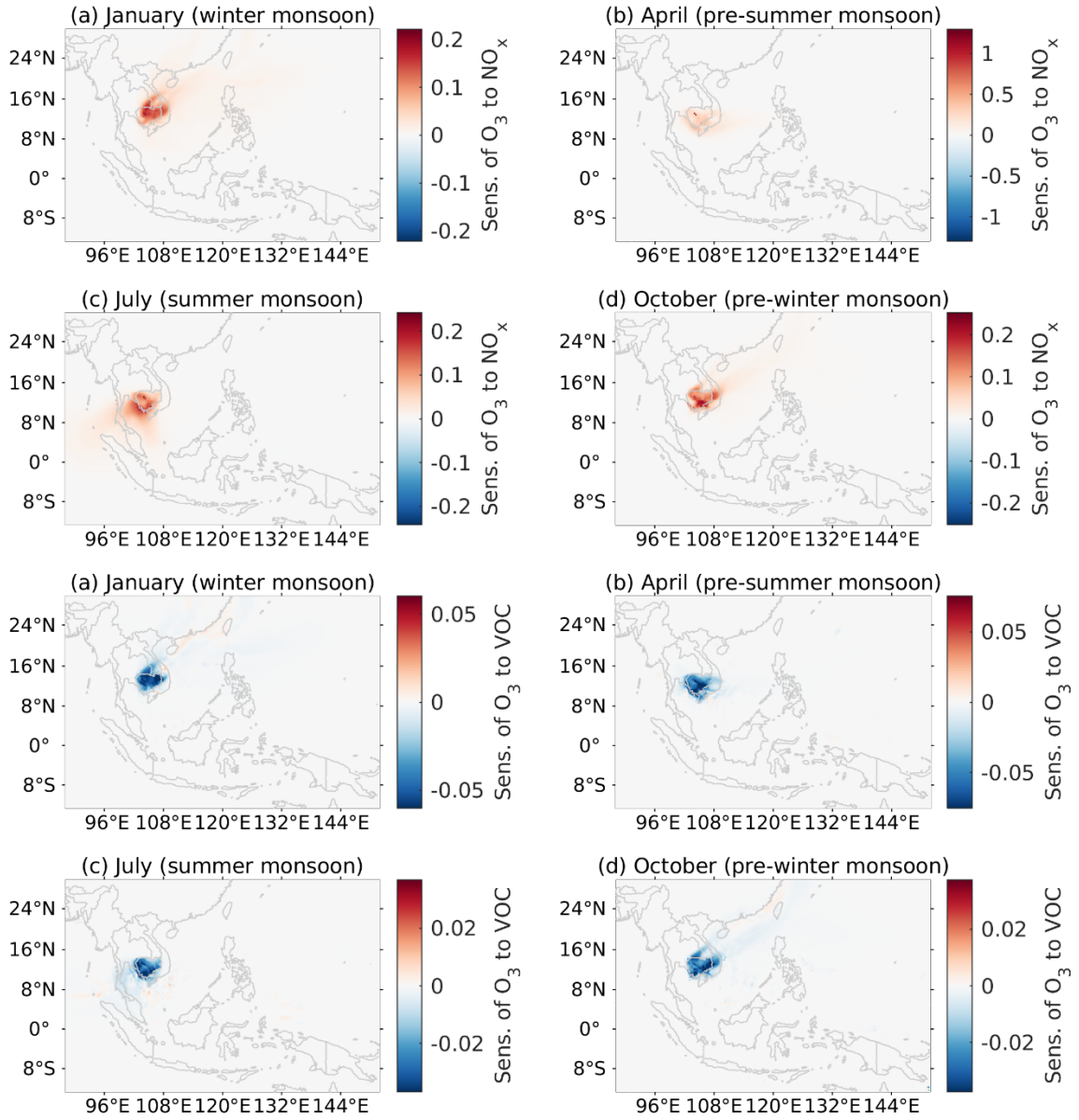

Fig. S30. Spatial distribution of the monthly mean sensitivity of O_3 in Cambodia to NO_x and VOC emissions during the four monsoon seasons.

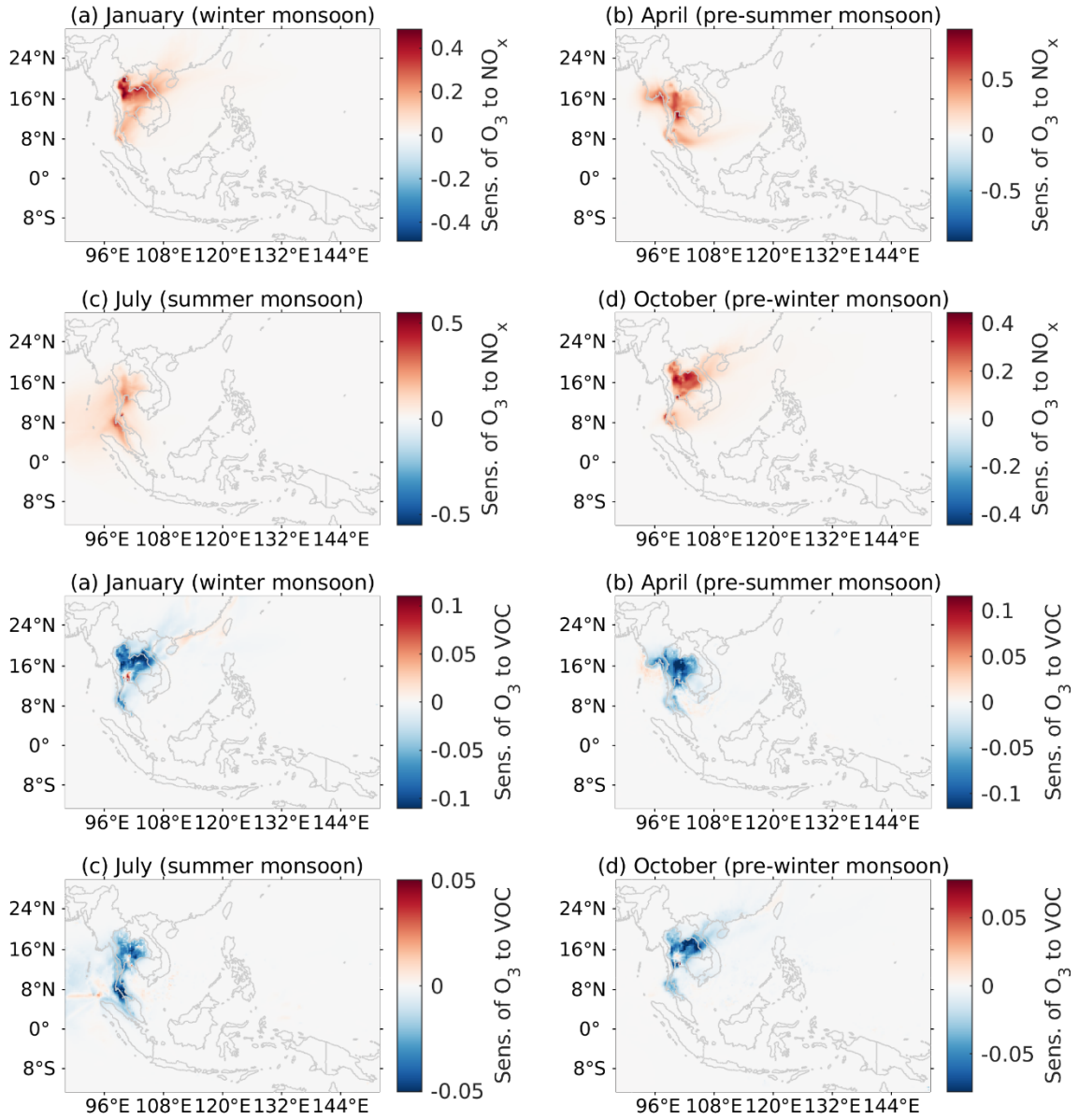

Fig. S31. Spatial distribution of the monthly mean sensitivity of O_3 in Thailand to NO_x and VOC emissions during the four monsoon seasons.

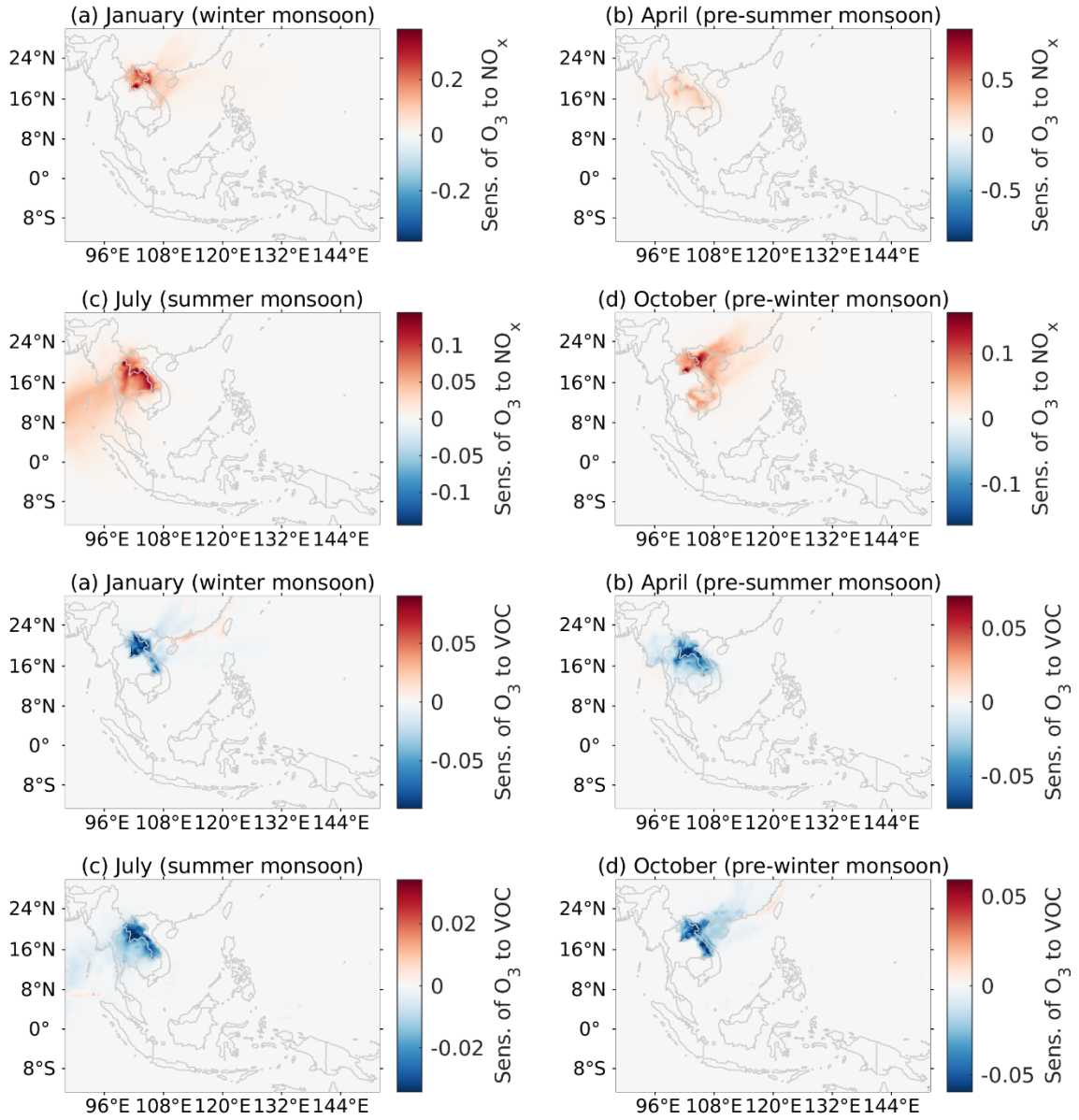

Fig. S32. Spatial distribution of the monthly mean sensitivity of O_3 in Laos to NO_x and VOC emissions during the four monsoon seasons.

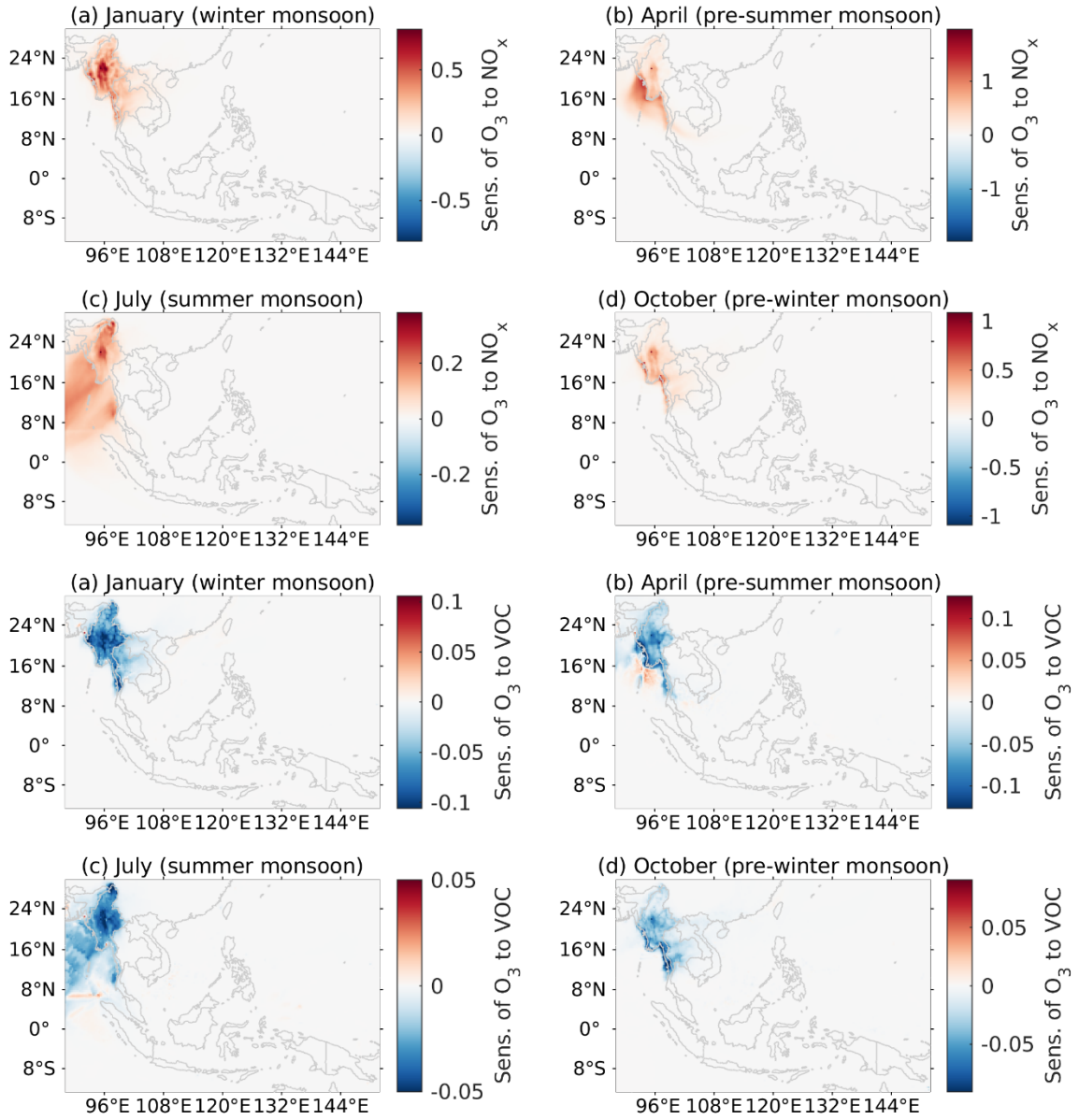

Fig. S33. Spatial distribution of the monthly mean sensitivity of O_3 in Myanmar to NO_x and VOC emissions during the four monsoon seasons.

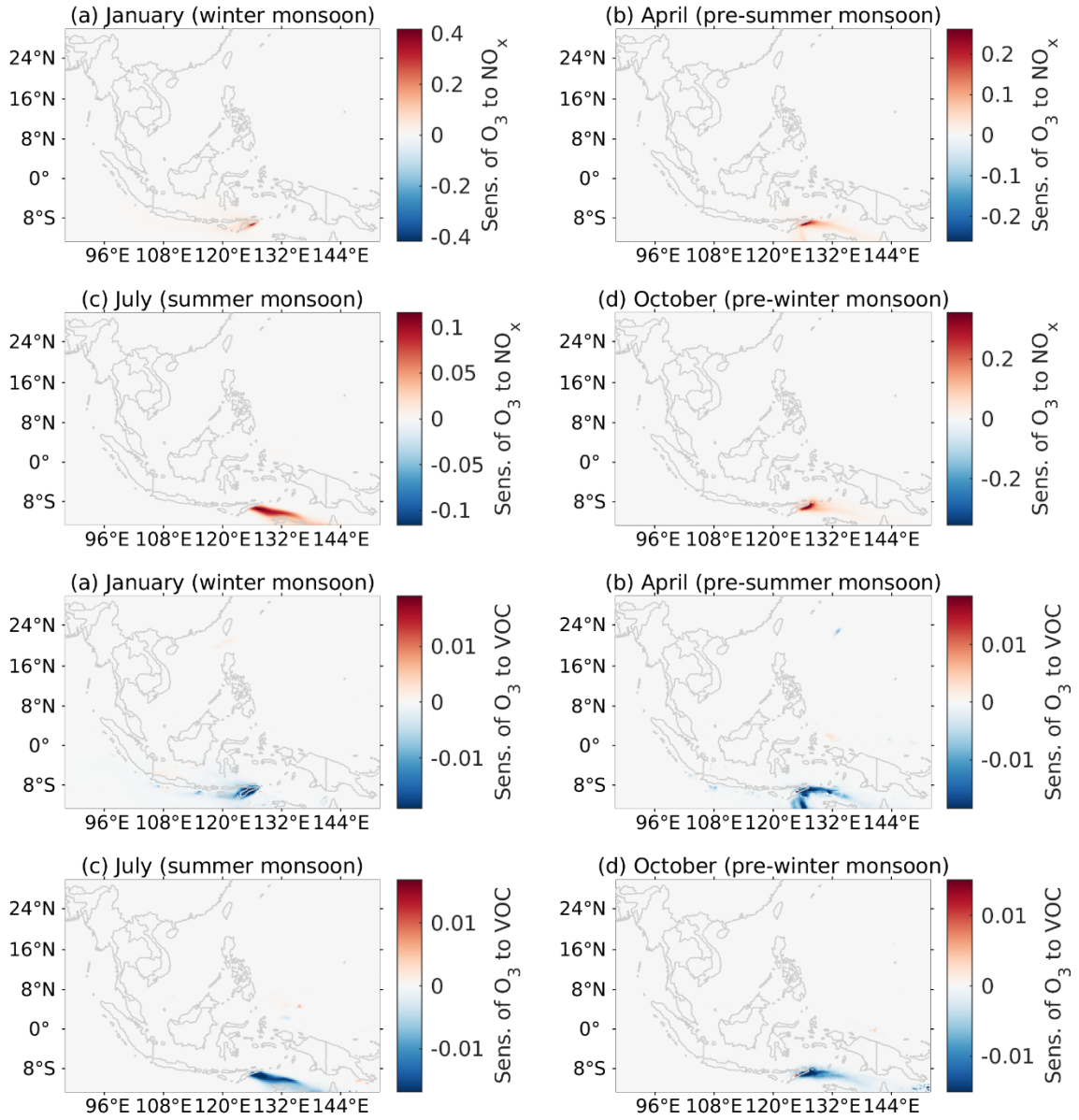

Fig. S34. Spatial distribution of the monthly mean sensitivity of O_3 in East Timor to NO_x and VOC emissions during the four monsoon seasons.

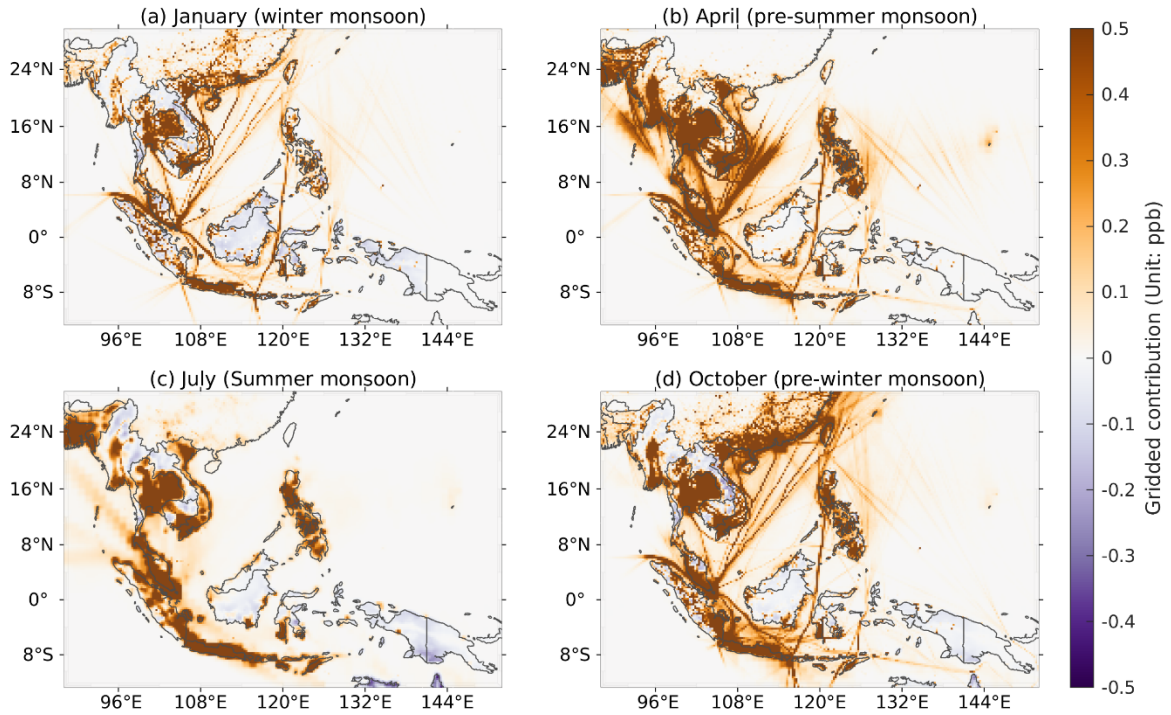

Figure S35. Grid-level contributions (unit: ppb) to the O_3 levels in Southeast Asia among four monsoon seasons.

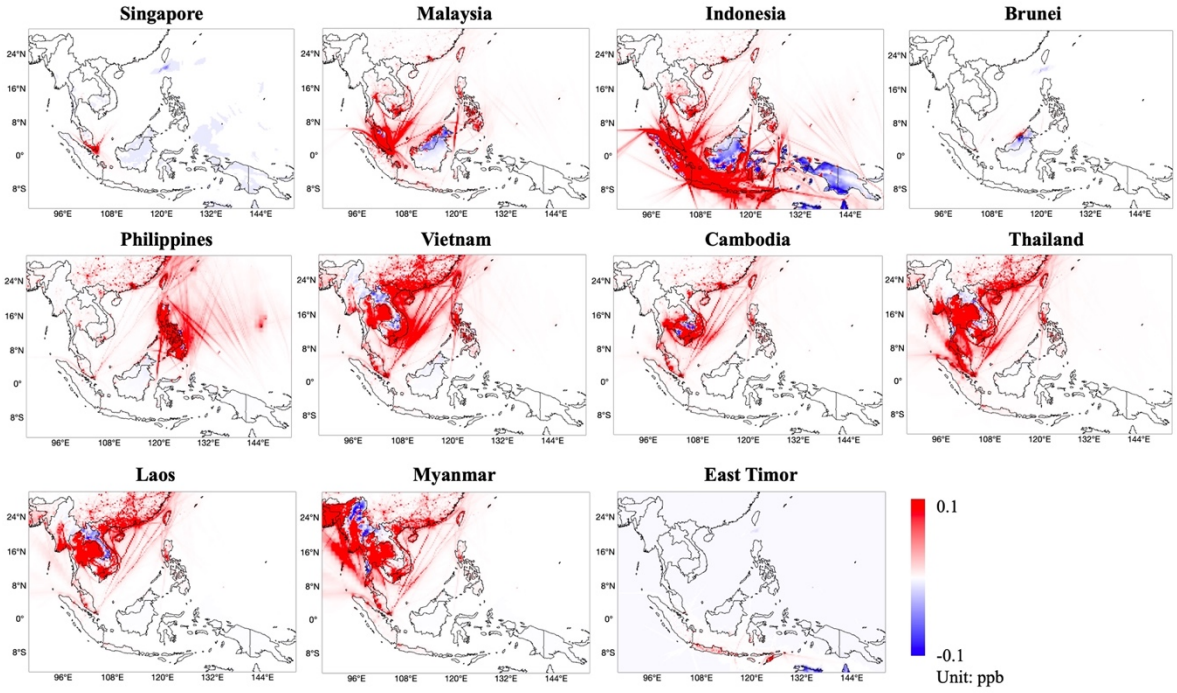

Figure S36. Grid-level contributions to the O_3 levels in different countries in Southeast Asia.

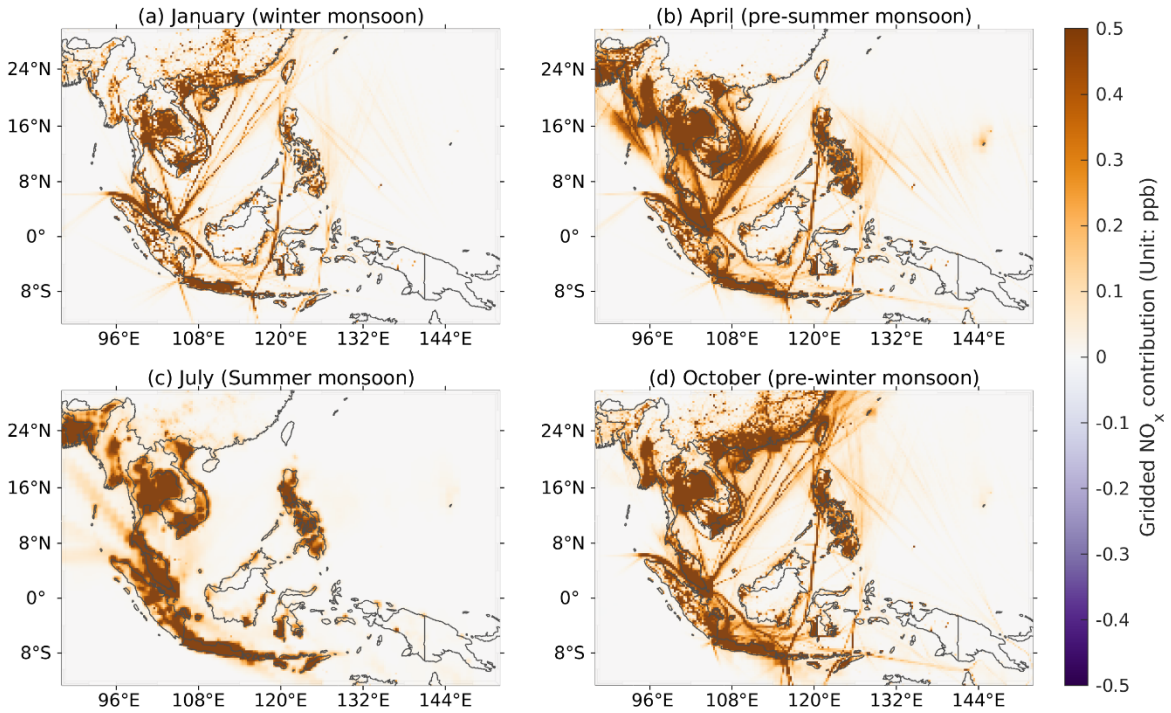

Figure S37. Grid-level NO_x contributions to the O_3 levels in different countries in Southeast Asia.

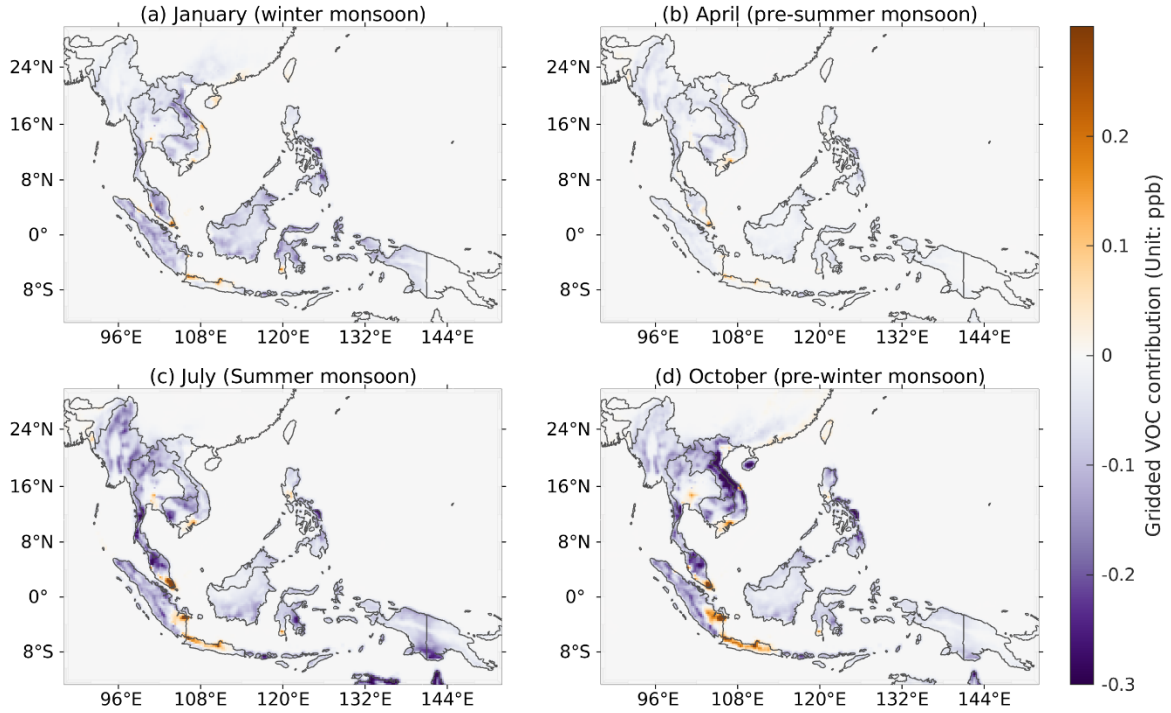

Figure S38. Grid-level VOC contributions to the O_3 levels in different countries in Southeast Asia.

Supplementary Tables

Table S1. Sensitivity test of MDA8 O_3 in January according to NO_x and VOC perturbations.

NOx perturbation	Original	-20% emissions	+20% emissions
	33.2	32.7	33.7
VOC perturbation	Original	-30% emissions	+30% emissions
	33.2	34.6	31.9

Table S2. VOC precursor emissions of CB05 in the CMAQ model.

Abbreviation	**Description**	**Abbreviation**	**Description**
ALDX	Aldehydes with 3 or more carbon atoms	OLE	Terminal alkene acids
BENZENE	Benzene	PAR	Carbon-carbon single bond
ISOP	Isoprene	TERP	Monoterpenes
ETH	Ethene	TOL	Toluene and other mono alkyl
ETHA	Ethane	XYL	Xylene
ETOH	Ethanol	ALD2	Acetaldehyde
FORM	Formaldehyde	MEOH	Methanol
IOLE	Internal alkene bond		

Table S3. Evaluation of the CMAQ model simulation by comparing the O_3 concentration levels with the ground-level measurements from different stations. Data sources include the EANET and the AQI databases.

Country	Stations	NMB (%)				RMSE (ppb)			
		Jan	Apr	Jul	Oct	Jan	Apr	Jul	Oct
Singapore (AQI)	Singapore	13.81	21.72	13.09	8.11	2.20	6.12	1.20	2.00
Brunei (AQI)	Muara	/	/	0.65	-1.48	/	/	0.98	2.07
	Pekan-Tutong	/	/	8.35	-3.91	/	/	0.81	1.52
Philippines (AQI)	Biñan city	/	/	/	21.60	/	/	/	2.93
Vietnam (AQI)	Hanoi	/	/	-1.22	24.08	/	/	2.65	7.71
	Quảng-ninh_phương nam	/	/	9.07	/	/	/	5.05	/
Thailand	Ayutthaya-witthayalai (AQI)	33.21	/	/	/	7.76	/	/	/
	Municipality office (AQI)	15.18	11.82	/	11.59	1.91	1.40	/	1.16
	Bangkok (EANET)	9.14	/	85.38	3.2	0.85	/	0.81	0.78
	Samutprakarn (EANET)	12.64	/	/	35.01	0.81	/	/	0.76
	Kanchanaburi (EANET)	/	12.83	/	/	/	0.76	/	/
	Chiang Mai (EANET)	-21.07	-42.23	35.46	/	0.69	1.13	0.67	/
	Nai Mueang (EANET)	/	-12.08	/	/	/	1.10	/	/
Cambodia (EANET)	Phnom Penh	/	/	/	-2.87	/	/	/	0.52
Malaysia (AQI)	balok-baru	/	/	-15.97	-23.67	/	/	2.41	2.98
	Bandaraya-melaka	/	/	-9.86	10.90	/	/	2.78	3.48
	Banting-selangor	/	/	0.93	14.01	/	/	2.51	3.30
	Batu-muda	/	/	11.05	24.24	/	/	2.97	4.49
	Batu-pahat	/	/	-12.83	5.54	/	/	3.10	2.76
	Jalan-tasek	/	/	-6.93	-14.30	/	/	2.33	2.23
	Kg. -air putih	/	/	25.85	5.10	/	/	4.64	2.89
	Nilai	/	/	1.34	15.38	/	/	2.44	3.63
	Pelabuhan-kelang	/	/	11.53	21.92	/	/	3.22	4.02
	Samalaju	/	/	-38.92	-36.39	/	/	7.27	3.85
	Segamat	/	/	-14.01	-9.86	/	/	3.23	2.49
	Seremban	/	/	4.39	9.47	/	/	2.61	2.87
	S-k Jalan Pegoh	/	/	-5.21	-3.11	/	/	2.35	2.28
	Tangkak	/	/	-15.22	-0.52	/	/	3.17	2.54

Table S4. The quantitative measurements of NMB, R, and IoA between our CMAQ simulation and the CAMS EAC4 reanalysis data over various Southeast Asian countries in 2019. MYS: Malaysia, IDN: Indonesia, BRN: Brunei, PHL: Philippines, VNM: Vietnam, KHM: Cambodia, THA: Thailand, LAO: Laos, MMR: Myanmar.

		MYS	IDN	BRN	PHL	VNM	KHM	THA	LAO	MMR
NMB	January	11.32	29.46	3.46	7.89	-1.08	-27.24	-9.41	-1.54	-30.73
	April	2.34	24.69	-16.90	-4.29	12.17	15.22	22.08	-10.14	-12.03
	July	-3.26	-10.94	-14.65	4.94	22.34	20.85	40.12	41.27	54.90
	October	4.67	-23.50	12.68	-6.00	-4.23	-18.46	4.33	-3.77	0.52
R	January	0.81	0.79	0.89	0.69	0.61	0.19	0.63	0.87	0.64
	April	0.81	0.82	0.81	0.61	0.24	0.33	0.42	0.18	0.43
	July	0.91	0.83	0.91	0.45	0.55	0.61	0.51	0.09	0.61
	October	0.89	0.69	0.91	0.62	0.52	0.71	0.34	0.79	0.73
IoA	January	0.88	0.75	0.94	0.72	0.78	0.42	0.75	0.93	0.69
	April	0.90	0.81	0.79	0.68	0.48	0.54	0.55	0.53	0.55
	July	0.95	0.88	0.86	0.66	0.64	0.54	0.52	0.31	0.45
	October	0.94	0.76	0.87	0.73	0.73	0.69	0.60	0.83	0.84

Table S5. The country-level MDA8 O_3 level (ppb) during the four monsoon seasons.

Country	Winter monsoon	Pre-summer monsoon	Summer monsoon	Pre-winter monsoon
Singapore	79.7	79.3	42.1	48.5
Malaysia	35.1	28.0	26.3	27.1
Indonesia	31.9	26.0	25.0	23.1
Brunei	26.1	20.8	15.1	19.4
Philippines	41.0	30.6	28.0	29.2
Vietnam	41.8	45.4	35.9	43.8
Cambodia	34.9	40.8	31.1	34.1
Thailand	39.2	45.6	36.0	41.4
Laos	33.0	36.2	30.8	33.3
Myanmar	23.4	36.4	32.9	27.8
East Timor	38.4	28.2	28.8	19.7

Table S6. Averaged height (m) of each layer in the model simulation.

Layer	**1**	**2**	**3**	**4**
Height (m)	25	37	59	82
Layer	**5**	**6**	**7**	**8**
Height (m)	106	133	165	202
Layer	**9**	**10**	**11**	**12**
Height (m)	247	301	365	442
Layer	**13**	**14**	**15**	**16**
Height (m)	532	641	770	923
Layer	**17**	**18**	**19**	**20**
Height (m)	1107	1325	1585	1896
Layer	**21**	**22**	**23**	**24**
Height (m)	2634	3559	5406	9050
Layer	**25**	**26**		
Height (m)	14412	19584		

Table S7. NO_x and VOC emissions from different sectors in the typical VOC-limited regions, including Singapore, Jakarta, Manila, Bangkok, Ho Chi Minh City, Hanoi, and Kuala Lumpur. TRA: transportation, SHP: shipping, IND: industry, RES: residential, FIR: fire, ENE: energy, REF: refinery, SLV: solvent, AGR: agriculture, BIO: biogenic emissions, SUM: summary of all emission sectors.

NO_x (mol/s)	Singapore	Jakarta	Manila	Bangkok	Ho Chi Minh City	Hanoi	Kuala Lumper
TRA	20.54	16.18	4.86	30.45	0.64	0.65	32.12
SHP	5.81	0.00	0.00	0.10	1.85	0.00	0.00
IND	12.24	5.82	6.48	9.23	0.26	0.13	4.90
RES	0.72	0.52	0.34	0.46	0.06	0.08	0.42
FIR	0.00	0.36	0.14	0.06	0.21	0.15	0.01
ENE	0.00	0.00	0.00	0.00	0.00	0.00	0.00
REF	0.19	0.04	0.01	0.32	0.00	0.00	0.02
SLV	0.00	0.00	0.00	0.00	0.00	0.00	0.00
AGR	0.23	0.21	0.15	0.04	0.06	0.07	0.11
BIO	0.00	0.00	0.00	0.00	0.00	0.00	0.00
SUM	39.74	23.12	11.98	40.66	3.09	1.07	37.58
VOC (mol/s)	Singapore	Jakarta	Manila	Bangkok	Ho Chi Minh City	Hanoi	Kuala Lumper
TRA	12.07	31.52	5.48	32.25	0.72	0.68	52.26
SHP	0.09	0.00	0.00	0.00	0.02	0.00	0.00
IND	7.73	3.72	2.74	13.53	0.09	0.07	3.80
RES	0.26	0.42	0.18	0.11	0.62	0.84	0.22
FIR	0.00	2.44	0.97	0.39	1.38	0.98	0.08
ENE	0.00	0.00	0.00	0.00	0.00	0.00	0.00
REF	0.92	4.29	18.62	96.62	0.10	0.11	9.73
SLV	31.13	15.97	17.61	17.38	0.18	0.21	27.62
AGR	1.48	0.61	0.73	1.72	0.00	0.00	2.33
BIO	22.50	15.12	22.75	13.56	26.99	22.64	53.36
SUM	76.19	74.09	69.08	175.57	30.11	25.54	149.39

Table S8. The contributions from the super-regional sources to the surface O_3 and the related premature mortality in Southeast Asia. For super-regional sources, we detailed the contributions from the super-regional emission transport and boundary conditions.

O_3 contribution (ppb)	Super-regional sources		
	Total	Boundary conditions	Super-regional emissions
Singapore	6.07	0.80	5.27
Malaysia	5.79	0.64	5.15
Indonesia	8.75	3.81	4.94
Brunei	4.80	0.38	4.42
Philippines	13.68	2.79	10.89
Vietnam	12.48	3.47	9.00
Cambodia	8.61	2.37	6.24
Thailand	10.73	3.99	6.74
Laos	12.28	4.60	7.68
Myanmar	14.93	10.01	4.93
East Timor	18.18	14.73	3.45

Table S9. NO_x and VOC emissions from different sectors in the typical NO_x-limited regions, including rural Malaysia, rural Indonesia, Mountainous Southeast Asia, and East Timor. TRA: transportation, SHP: shipping, IND: industry, RES: residential, FIR: fire, ENE: energy, REF: refinery, SLV: solvent, AGR: agriculture, BIO: biogenic emissions, SUM: summary of all emission sectors.

NO_x (mol/s)	Rural Malaysia	Rural Indonesia	Mountainous Southeast Asia	East Timor
TRA	0.41	0.14	0.27	0.11
SHP	0.22	0.02	0.02	0.00
IND	0.04	0.04	0.10	0.01
RES	0.01	0.02	0.03	0.01
FIR	0.01	0.04	0.07	0.02
ENE	0.00	0.00	0.00	0.00
REF	0.00	0.00	0.00	0.00
SLV	0.00	0.00	0.00	0.00
AGR	0.02	0.02	0.03	0.02
BIO	0.00	0.00	0.00	0.00
SUM	0.72	0.29	0.53	0.16
VOC (mol/s)	Malaysia	Indonesia	Mountainous Southeast Asia	East Timor
TRA	0.35	0.18	0.22	0.17
SHP	0.00	0.00	0.00	0.00
IND	0.03	0.03	0.07	0.01
RES	0.05	0.30	0.28	0.10
FIR	0.06	0.27	0.45	0.10
ENE	0.00	0.00	0.00	0.00
REF	0.10	0.03	0.32	0.01
SLV	0.29	0.20	0.20	0.06
AGR	0.02	0.00	0.01	0.00
BIO	51.19	33.53	29.67	13.48
SUM	52.08	34.55	31.22	13.93

Reference

Jin, X., Fiore, A. M., Murray, L. T., Valin, L. C., Lamsal, L. N., Duncan, B., ... & Tonnesen, G. S. (2017). Evaluating a space-based indicator of surface ozone-NOx-VOC sensitivity over midlatitude source regions and application to decadal trends. *Journal of Geophysical Research: Atmospheres*, *122*(19), 10-439.